Measurement of the Higgs boson in decays to bosons using the ATLAS detector

Dongshuo Du

Shandong University

(On behalf of the ATLAS collaboration)

XXVIII International Workshop on Deep-Inelastic Scattering and Related Subjects
Virtual Event @ Stony Brook University, April 12-16, 2021

Outline

- Overview of Higgs physics in diboson final states
- Property measurement
  - Higgs mass measurement in ZZ* decay channel
- Higgs boson cross sections measurement
  - Measurement of Simplified Template Cross Section (STXS) in $H\rightarrow WW^*$, $H\rightarrow ZZ^*$ and $H\rightarrow\gamma\gamma$ decay channels
  - Fiducial inclusive and differential cross-section measurements in $H\rightarrow ZZ^*$ and $H\rightarrow\gamma\gamma$ decay channels
- Summary

Higgs Physics In Diboson Final States

- The most prolific decay: H →bb (58%), very hard to observe
- The branching ratios (BR) of H → WW*(→lvlv) /ZZ*(→4l)/γγ are 1.0%, 0.012% and 0.23%, respectively
- The final states (e, μ, γ) are very sensitive & leave a clean signature in the ATLAS detector
  - H→ZZ*→4l and H →γγ : the most sensitive channels for observation
    - H→ZZ*→4l, S/B > 2
    - H→γγ, S/B ~5%
  - H→ WW*→lvlv (high yield with fair S/B)
    - Larger branching ratio
    - Clean signature
    - High background

⟹ Powerful tool for measuring the Higgs properties

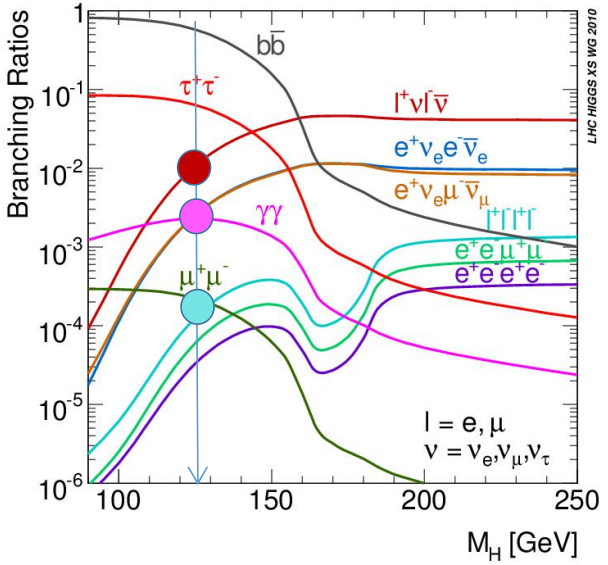

Higgs Mass Measurement

ATLAS-CONF-2020-005

- Full Run2 dataset @13TeV, integrated luminosity of 139 fb^{-1}
- H→ZZ*→4l, (4e, 4μ, 2e2μ and 2μ2e final states)
  - **Best for Higgs mass measurement** (statistics dominated)
  - The uncertainty on the mass depends on the mass resolution.
- Improve resolution:
  - ➢ A kinematic fit the invariant mass of the leading lepton pair to the Z boson mass;
  - ➢ Final-state radiation (FSR) photons included in the mass computation;
  - ➢ Consider the invariant mass resolution of the four-lepton system on a per-event basis.
  - ➢ 4 BDT bins to further distinguish signal from ZZ*

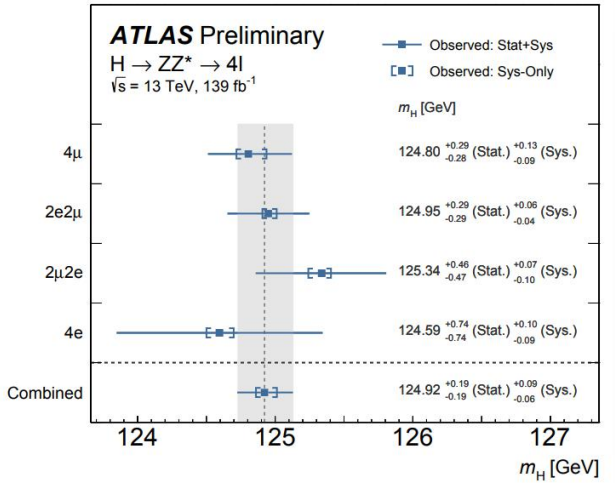

- ➢ Extracted via profile likelihood fit to 16 analysis categories
- ➢ Combined results: $m_H = 124.92^{+0.21}_{-0.20}\,GeV$
- ➢ Statistically limited channel

Simplified Template Cross Section (STXS)

- The aim with STXS method:
  - Improve sensitivity of measurements
  - Reduce their dependence on the theory
  - High p_T^H bins more sensitive to beyond standard model (BSM) effects

- STXS framework provides different stages (e.g. stage 0, stage 1, stage 1.2) with varying degrees of granularity

- Categorising events into bins of key (truth) variables (p_T^H, N_{jets}, m_{jj}) in different production modes (ggH, qqH, VH and ttH)

- STXS well-suited to combine different decay channels

- Higgs boson properties measured with 139 fb^{-1} ($\sqrt{s}$ = 13 TeV) for Higgs boson rapidity $|y_H| < 2.5$

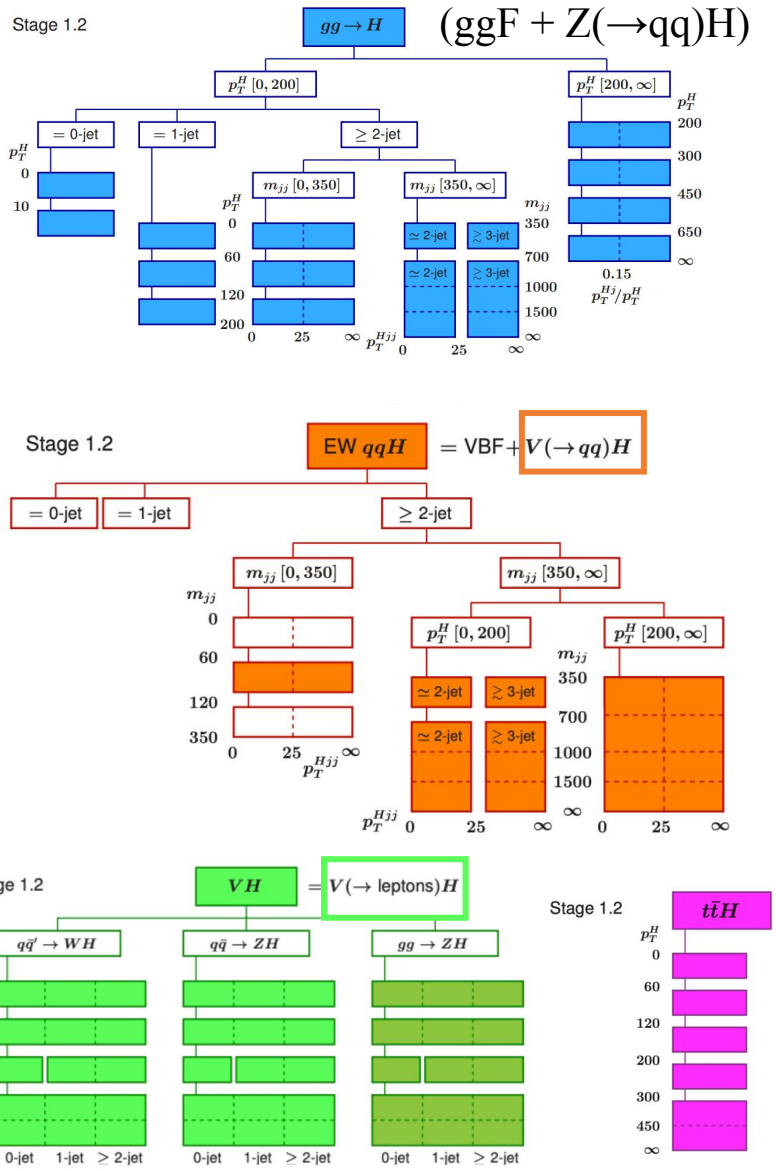

H→WW*: Analysis Strategy

- Full Run2 dataset @13TeV, integrated luminosity of 139 fb^{-1}
- Signal: different flavour (eμ+μe) opposite charge leptons + MET
- Events split in 4 analysis categories based on N_{jets}(*)
  - ggF: $N_{jets} = 0,1, \geq 2$, cut based
    - m_T used as discriminant variable
  - VBF: $N_{jets} \geq 2$, "deep" neural network (DNN) based
    - DNN used as discriminant variable
- Main background:
  - Non-resonant qqWW, top and Z→ττ
    - ggF: qqWW, top and Z→ττ normalized by control regions (CR)
    - VBF: top and Z→ττ normalized by CRs
  - Background with mis-identified leptons estimated by data-driven fake factor method

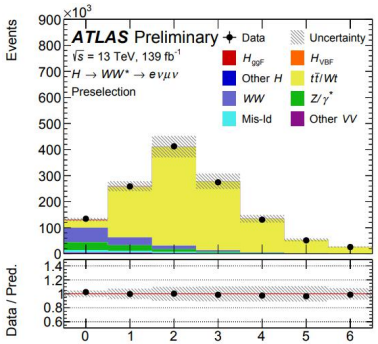

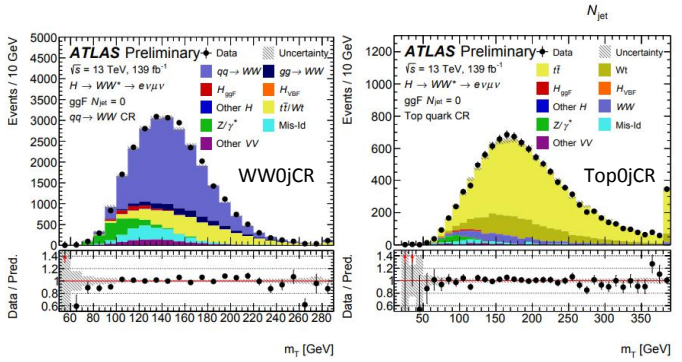

ATLAS-CONF-2021-014

(*) Full event selection in the backup

$$m_T = \sqrt{(E_T^{\ell\ell} + E_T^{miss})^2 - |\boldsymbol{p}_T^{\ell\ell} + \boldsymbol{E}_T^{miss}|^2}, \quad E_T^{\ell\ell} = \sqrt{|\boldsymbol{p}_T^{\ell\ell}|^2 + m_{\ell\ell}^2}$$

H→WW*: STXS

ATLAS-CONF-2021-014

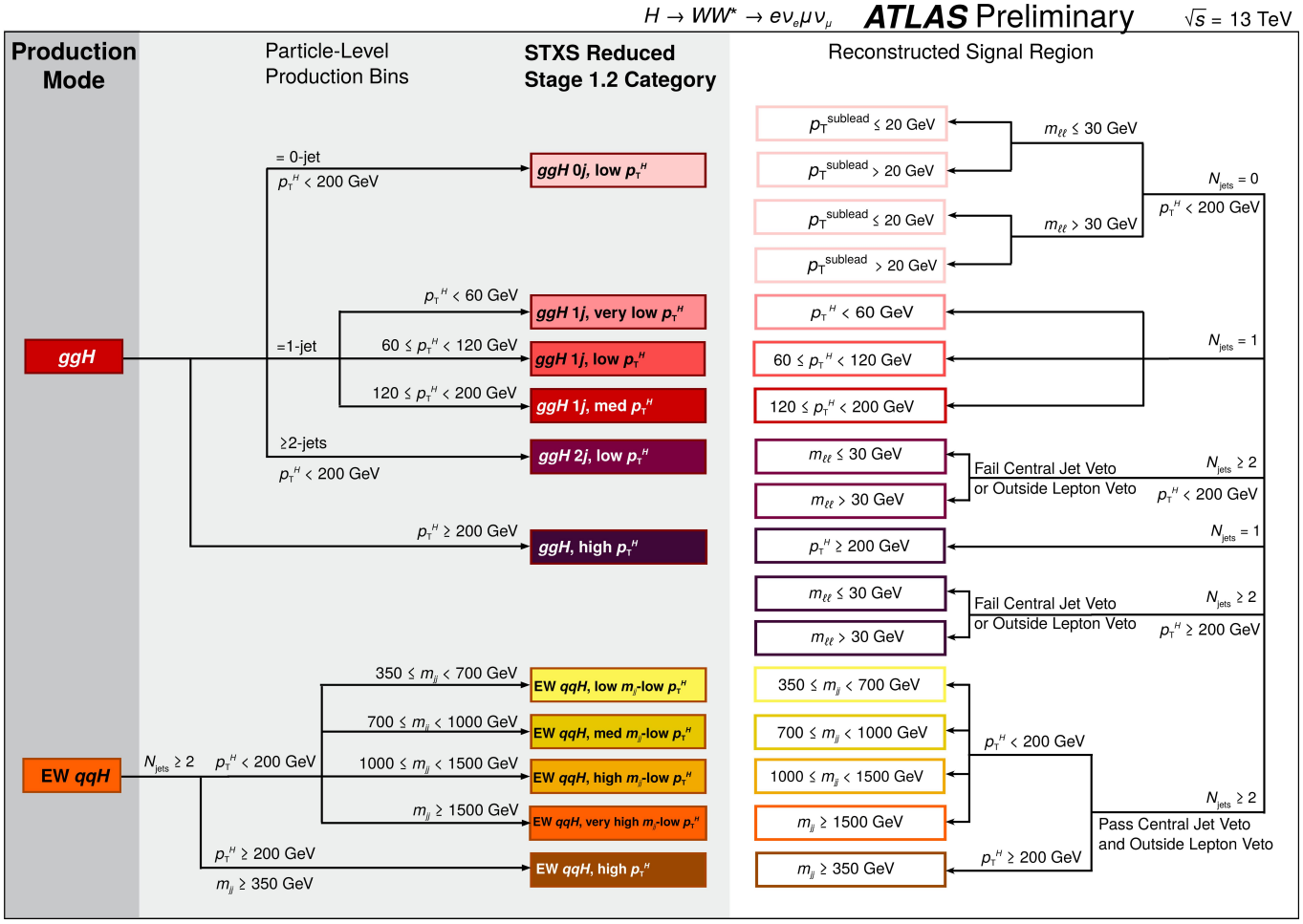

- Split by p_T^H, N_{jets}, m_{jj} into 11 categories
- 17 signal regions (SR)
- 27 control regions (CR)

- This analysis based on the reduced stage 1.2 category to ensure sensitivity for all measurements.
- CRs split similar to SRs where statistics allow

$$p_T^H = |\boldsymbol{p}_T^{\ell\ell} + \boldsymbol{E}_T^{\text{miss}}|$$

H→WW*: Results

ATLAS-CONF-2021-014

Coupling results

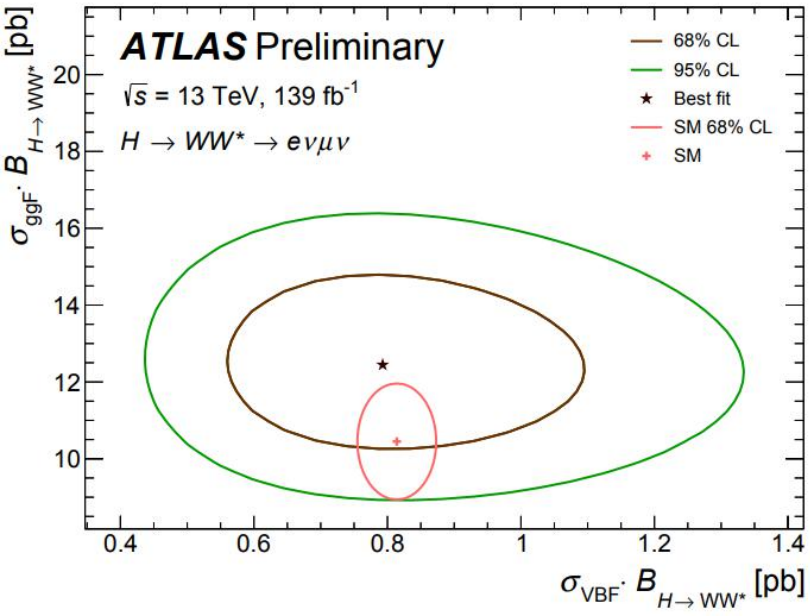

$\sigma_{ggF} \cdot \mathcal{B}_{H\to WW^*} = 12.4 \pm 1.5$ pb

$= 12.4 \pm 0.6\,(\text{stat.}) \pm 0.9\,(\text{exp syst.})\,^{+0.7}_{-0.6}\,(\text{sig theo.}) \pm 1.0\,(\text{bkg theo.})$ pb

$\sigma_{VBF} \cdot \mathcal{B}_{H\to WW^*} = 0.79\,^{+0.19}_{-0.16}$ pb

$= 0.79\,^{+0.11}_{-0.10}\,(\text{stat.})\,^{+0.06}_{-0.05}\,(\text{exp syst.})\,^{+0.13}_{-0.09}\,(\text{sig theo.})\,^{+0.08}_{-0.06}\,(\text{bkg theo.})$ pb,

- Compatible with SM predictions within 1 σ

STXS results

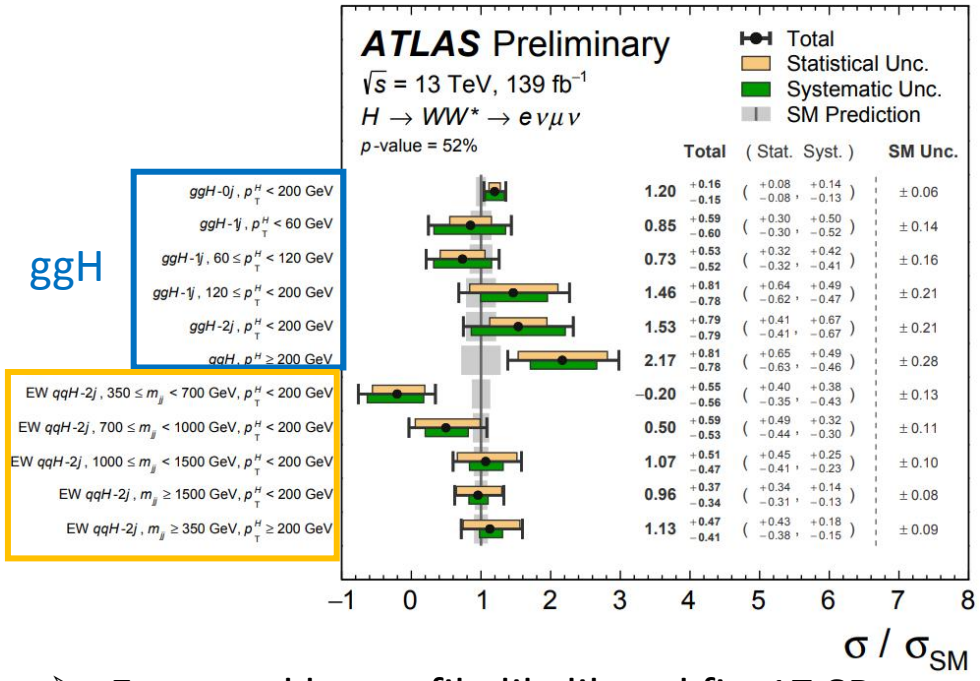

- Extracted by profile likelihood fit: 17 SRs (m_T/DNN) + 27 CRs
- ggH uncertainties limited by both stat. + syst. uncertainty
- qqH uncertainties limited by statistical uncertainty at high m_{jj} / p_T^H
- Compatible with the SM predictions with a p-value of 52%

H→ZZ*→4ℓ: Four-lepton Invariant Mass Distribution

Analysis features：

- **Small branching fraction （ 0.0124% at m_H = 125 GeV ）**
- **Best final S/B ratio, better than 2:1**
- **Clean signature with fully reconstructed final state**
- **good mass resolution = 1-2%**

Full Run2 dataset @13TeV, integrated luminosity of 139 fb^{-1}

Signal: 4 leptons (4e, 4μ, 2e2μ and 2μ2e)

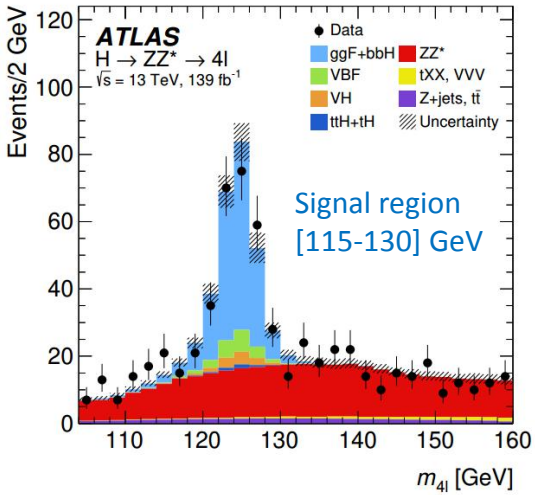

Eur. Phys. J. C 80, 957 (2020).

Backgrounds:

- Irreducible background for ZZ*/Zγ*, the normalisation constrained with a data-driven technique .
  - obtained from data by using the mass interval with 105–160 GeV
- Reducible background with non-prompt leptons for Z+jets, tt+jets, Zjets, WW+jets, and WZ+jets estimated from data.

Multivariate discriminants using neural networks used to separate ggF from ZZ* background, and to separate the production modes ggF/VH/VBF for 1 and 2 jets reconstruction categories

H→ZZ*→4ℓ: Production Mode Cross Sections

Eur. Phys. J. C 80, 957 (2020).

Production Mode Stage

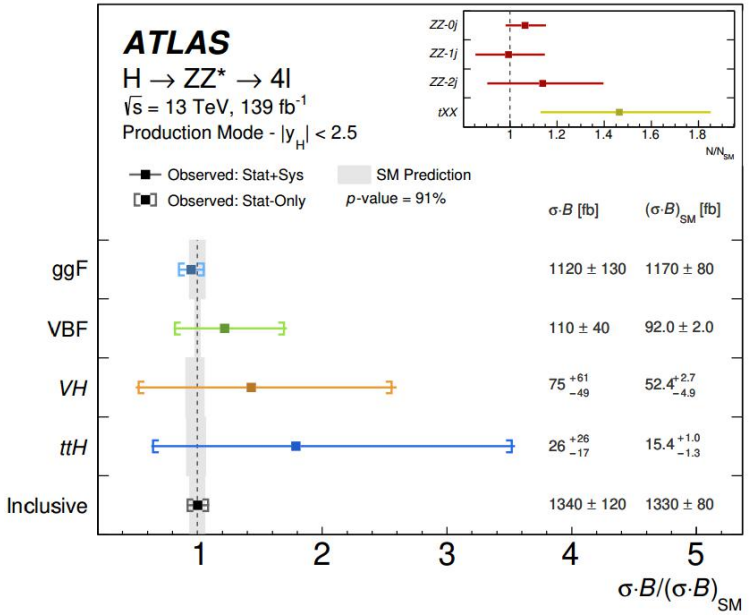

Reduced Stage 1.1

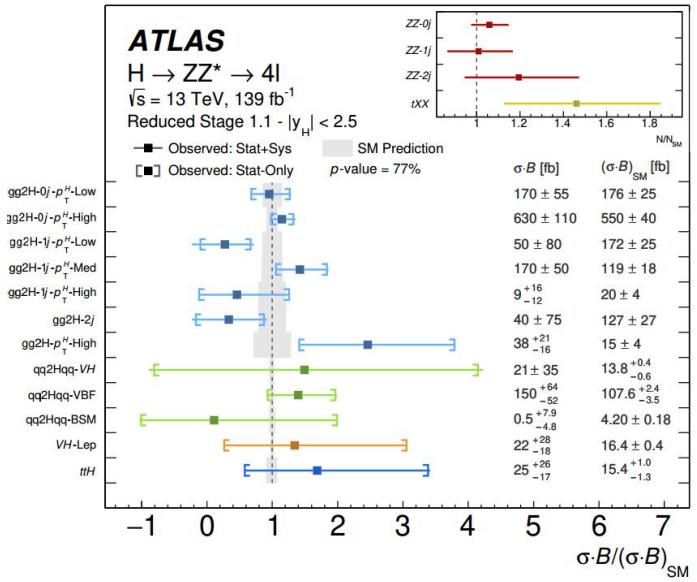

- The inclusive H→ZZ* production cross-section for $|y_H| < 2.5$:
  1.34 ± 0.12 pb
- Good agreement with the SM predictions:
  1.33 ± 0.08 pb

- Compatible with SM predictions with a p-value of 77%.
- Due to finer categorisation, results are statistically limited.

H→γγ: Diphoton Invariant Mass Distribution

Analysis features：

- Fairly high branching fraction **wrt** H→ZZ*→4ℓ**: ~20 times larger**
- **Fair final S/B-ratio: about 1:20**
- **Excellent performance of photon reconstruction and identification**
- **Final states are fully reconstructable**
- **Good mass resolution = 1-2%**

ATLAS-CONF-2020-026

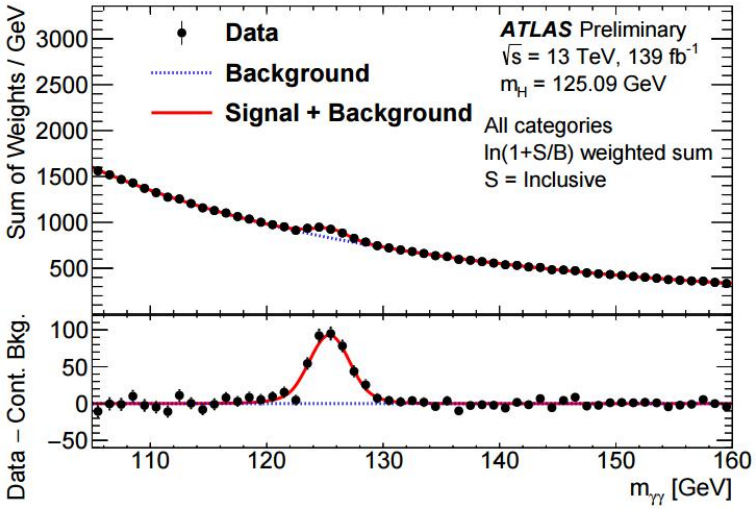

Signal + background model fit for all categories, and the residual plot after subtracting the backgrounds

Full Run2 dataset @13TeV, integrated luminosity of 139 fb^{-1}

Signal: diphoton

Backgrounds:

- SM diphoton production or γ+jets, jet+jets (estimated from data)

H→γγ: Production Mode Cross Sections

ATLAS-CONF-2020-026

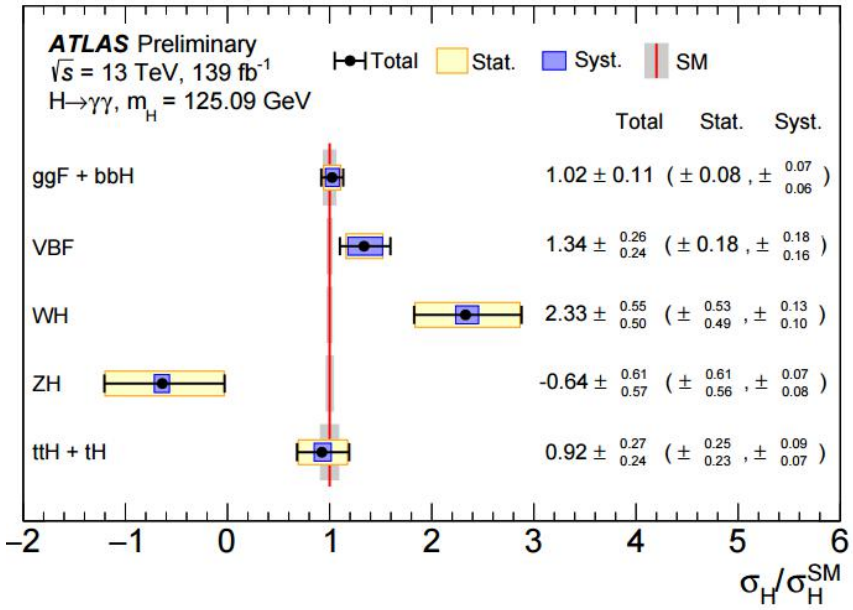

- Good agreement with SM prediction for ggF+bbH and ttH+tH measurements
- VBF is about 1.4 σ higher than SM prediction
- The combined cross section of WH and ZH(VH) is consistent with SM prediction.

$\sigma_{VH} = 5.9 \pm 1.4\,\text{fb}$ versus $\sigma_{VH,\text{exp}} = 4.53 \pm 0.12\,\text{fb}$

- The inclusive H→γγ production cross-section for $|y_H| < 2.5$:

$$(\sigma \times B_{\gamma\gamma})_{\text{obs}} = 127 \pm 10\,\text{fb}$$

- Good agreement with the SM predictions:

$$(\sigma \times B_{\gamma\gamma})_{\text{exp}} = 116 \pm 5\,\text{fb}.$$

H→γγ: STXS

ATLAS-CONF-2020-026

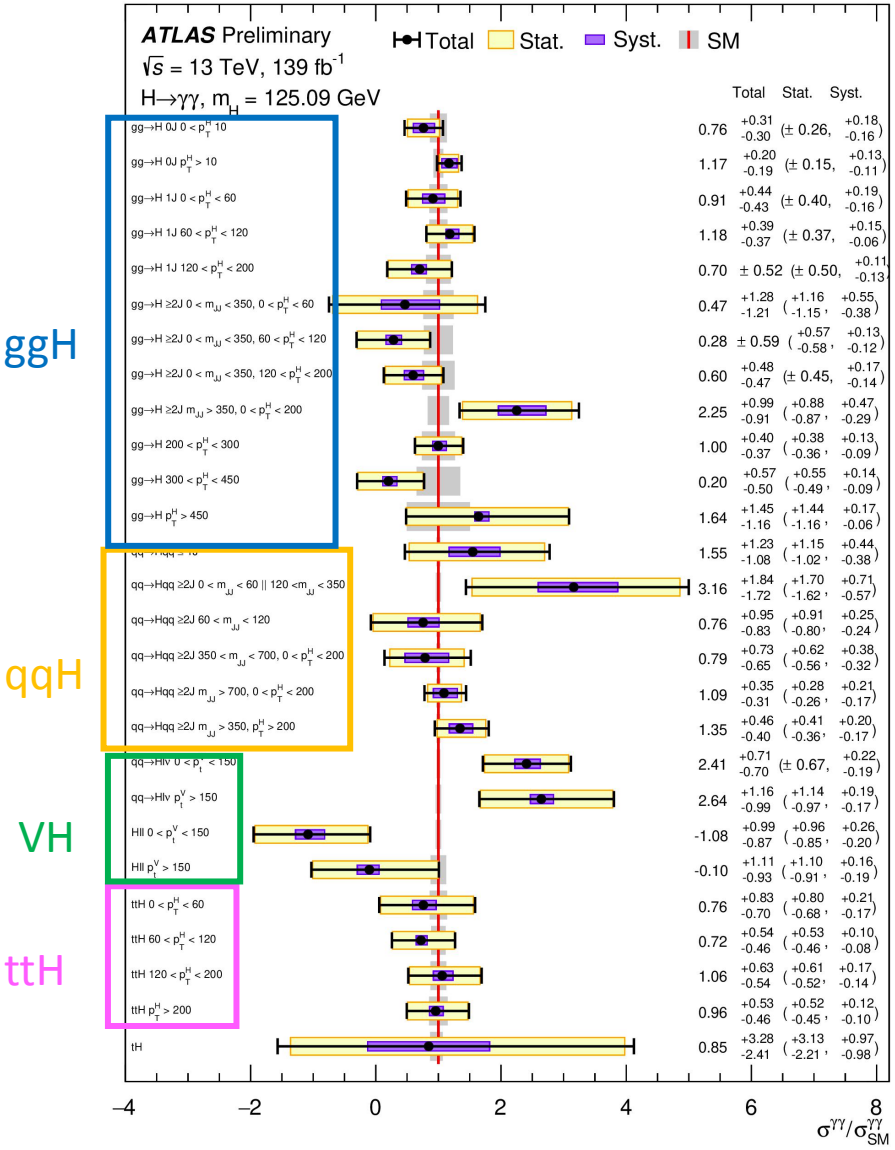

- More statistics with Full Run2 dataset, finer binning expecially for non-ggH production mode.
- Cross-sections of 27 STXS regions are measured
  - First to measure ttH differentially
- In general, measurements are compatible with SM predictions
- Due to finer categorisation, measurements are statistically limited.

Differential and Fiducial Cross Sections

- Measured in fiducial volume: a restricted truth phase space used for a cross section measurement
  - Minimise model-dependent acceptance extrapolations → The fiducial selection defined closely match the selection requirements of detector-level analysis

$$\sigma^{\text{fid}} = \sigma^{\text{Total}} \times \text{A} \times BR = \frac{N_s}{C \times L_{\text{int}}}$$

N_s : number of observed signal events, $C = \frac{N_{Rec}}{N_{Fid}}$: the correction factor for detector efficiency and resolution effect, L_{int} : Integrated luminosity

- Inclusive fiducial cross-section: No attempt to separate Higgs production/decay modes → compare with best available predictions in the detector phase space

- Differential cross-section: Measure differential cross section as a function of Higgs p_T , N_{jets}…
  - The Higgs p_T distribution can test couplings to b and c quarks, and high pt can tests new physics.
  - The jet multiplicity is sensitive to different production mechanisms and the theoretical modelling of high-quark and gluon emission.

H→ZZ*→4ℓ: Inclusive and Differential Cross Section

Eur. Phys. J. C 80, 942 (2020)

- H→ZZ*→4ℓ decay mode provides excellent resolution for Higgs kinematic variables
- Fitting 4ℓ distribution in each final state (right) or **differential bin** (bottom)to extract the measured cross section

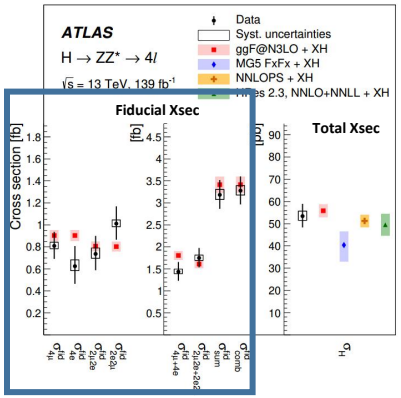

Inclusive fiducial cross section:

$$\sigma_{\text{fid}} = 3.28 \pm 0.30\,(\text{stat.}) \pm 0.11\,(\text{syst.})\ \text{fb}$$

$$\sigma_{\text{fid},SM} = 3.41 \pm 0.18\ \text{fb}$$

The measurement has precision at 10% level

Good agreement with LHCXSWG prediction

Low p_T^H test couplings to b and c quarks and High p_T^H test BSM

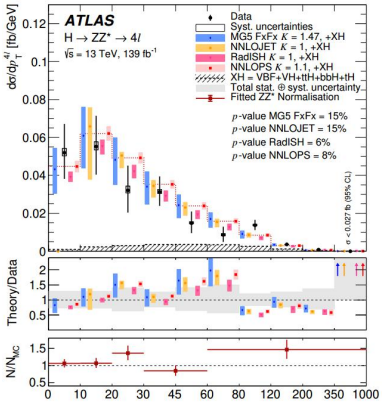

$|y_{4l}|$→ test gluon PDFs

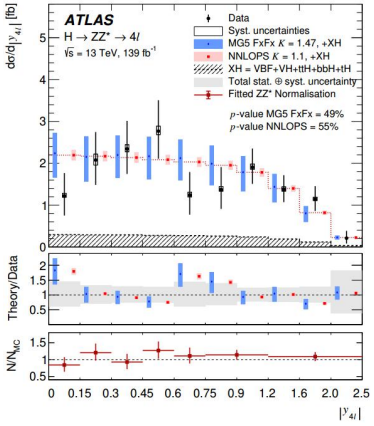

Sensitive to BSM physics

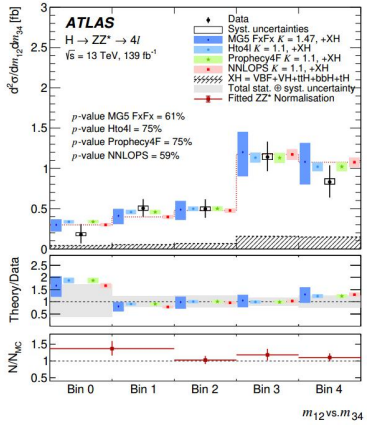

Measured cross sections in good agreement with SM predictions within uncertainties

Limited by statistical uncertainties

H→γγ: Inclusive and Differential Cross Section

ATLAS-CONF-2019-029

- Excellent performance of photon reconstruction and identification
  → **good resolution for Higgs variables**
- The H → γγ signal yields are extracted from fits to the diphoton invariant mass spectrum

Inclusive fiducial cross section:

$$\sigma_{\text{fid}} = 65.2 \pm 7.1\,\text{fb}$$

$$\sigma_{\text{fid},SM} = 63.6 \pm 3.3\,\text{fb}$$

The measurement has precision at 11% level

Differential cross-section still limited by statistical uncertainties

Low p_T^H test couplings to b and c quarks and High p_T^H test BSM

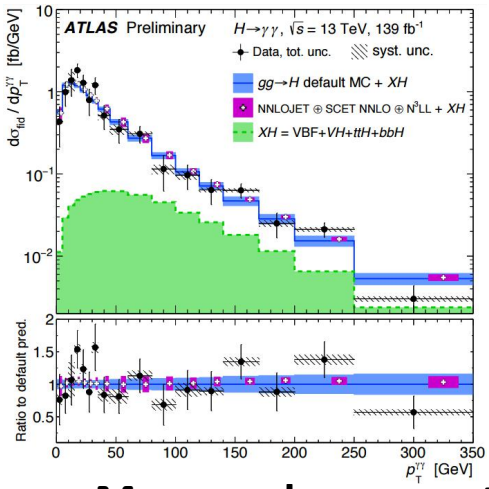

N_{jets} → test modelling of radiations at high pT and production modes

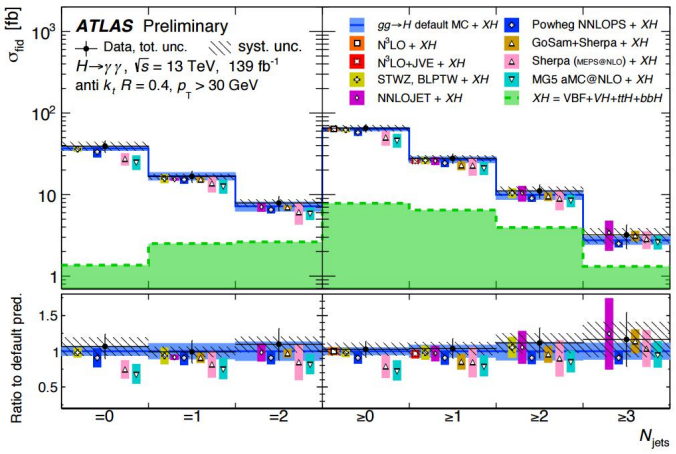

$|y_{4l}|$→ test gluon PDFs

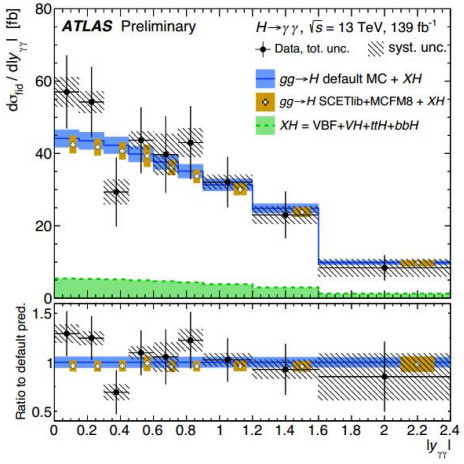

Measured cross sections in good agreement with SM predictions within uncertainties

Summary

- $H \rightarrow ZZ^*$, $H \rightarrow \gamma\gamma$, $H \rightarrow WW^*$ channels investigated with 139 fb^{-1} of data collected with the ATLAS detector @13TeV
  - Inclusive, STXS and differential cross section measurements are presented
  - all the measurements are in agreement with the SM predictions
- Thanks to the increased statistics with full Run2 dataset, more finely-grained measurements are presented.

Stay tuned for more results to come from Run2

Thank you for your attention

Back up

Higgs Physics In Diboson Final States

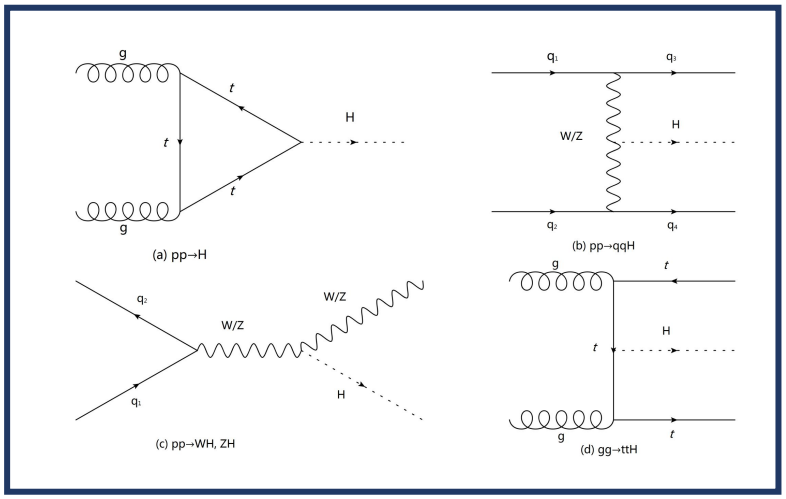

Production modes

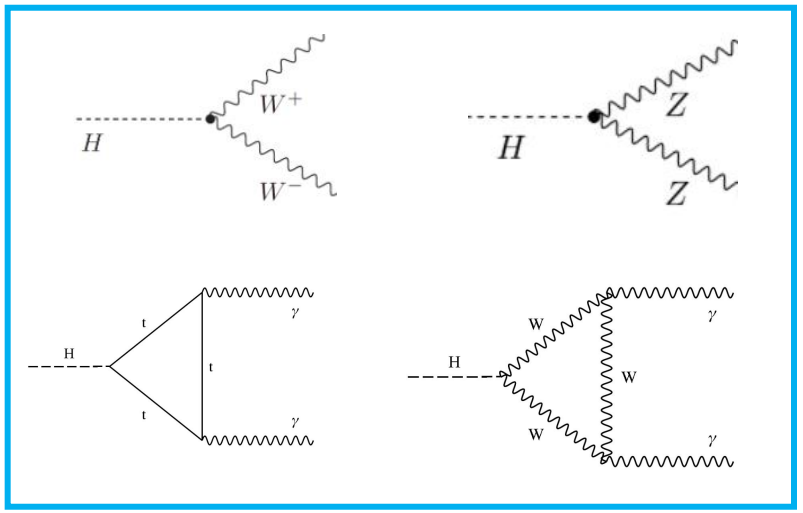

Higgs decay to diboson

- The most prolific decay: H →bb (58%), very hard to observe
- The branching ratios (BR) of H → WW*(→lvlv) /ZZ*(→4l)/γγ are 1.0%, 0.012% and 0.23%, respectively
- The final states (e, μ, γ) are very sensitive & leave a clean signature in the ATLAS detector

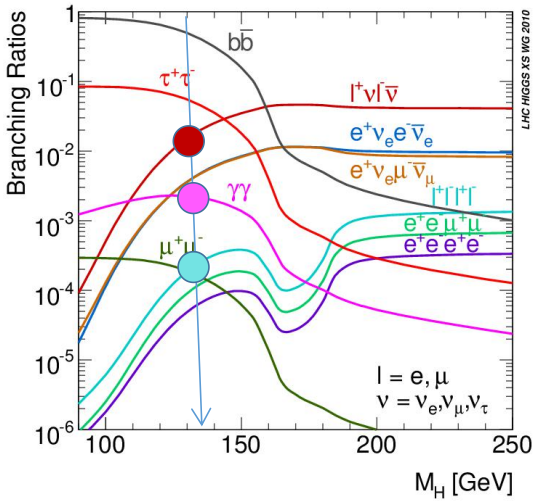

Higgs mass measurement

Process	Generator	PDF
$qqZZ$	SHERPA v2.2.2 [68–71]	NNPDF3.0nnlo
$qqZZ$ (alternate)	POWHEG-BOX v2	CT10
$qqZZ$ (alternate)	MADGRAPH5_aMC@NLO	PDF4LHC (NLO)
$ggZZ$	SHERPA v2.2.2	NNPDF3.0nnlo
EW ZZ	SHERPA v2.2.2	NNPDF3.0nnlo
WZ	POWHEG-BOX v2	CT10
Z+jets	SHERPA v2.2.1	NNPDF3.0nnlo
$t\bar{t}$	POWHEG-BOX v2	NNPDF3.0nnlo
tXX	MADGRAPH5_aMC@NLO	NNPDF3.0nnlo
VVV	SHERPA v2.2.2	NNPDF3.0nnlo

VVV: ZZZ, WZZ, and WWZ

tXX: one or more top quarks or electroweak bosons: tW Z, ttbarW^+W^-, ttbart , ttbarttbar and tZ

Higgs mass measurement

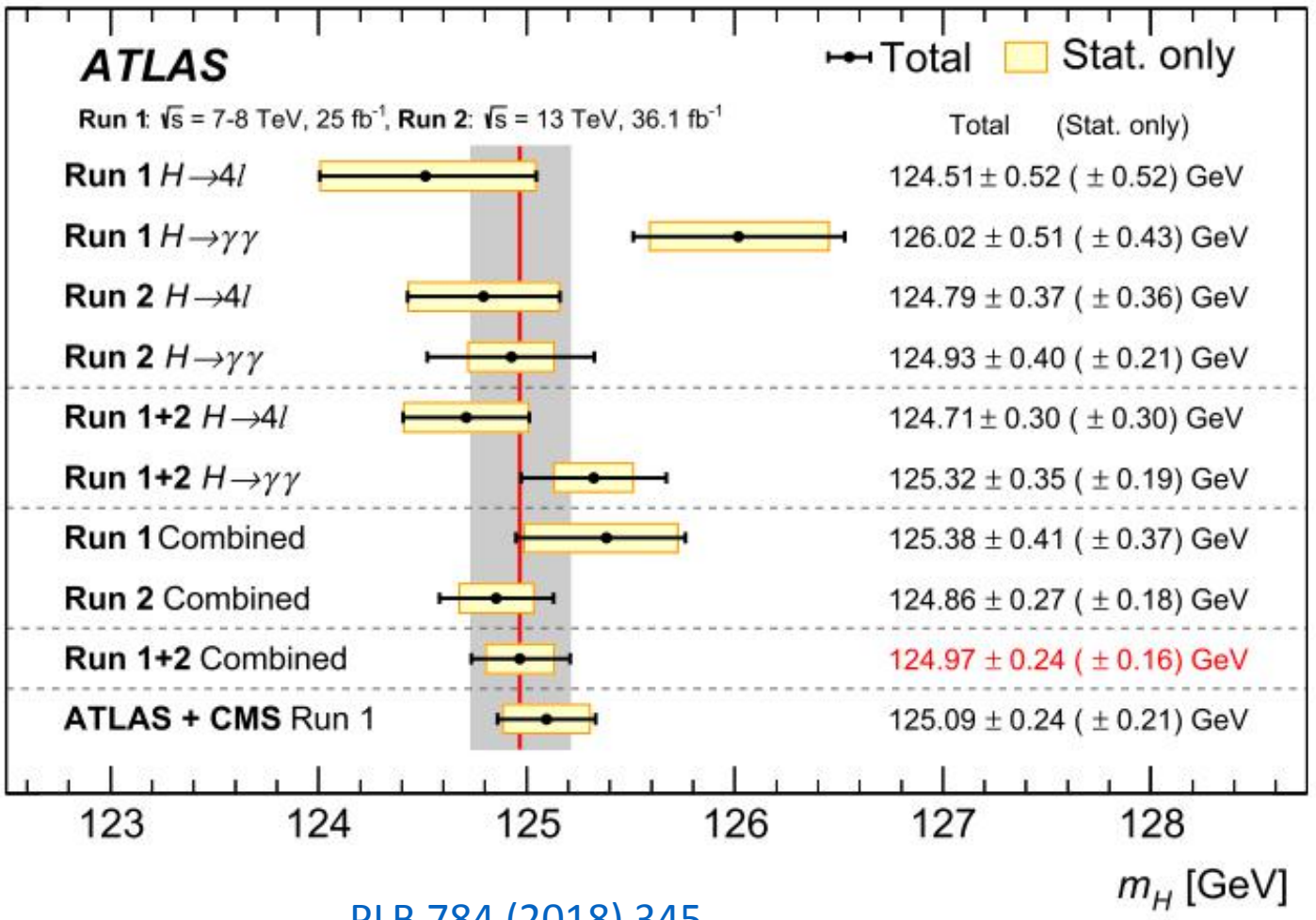

PLB 784 (2018) 345

Higgs mass measurement

- BDT inputs: The transverse momentum and pseudorapidity of the four-lepton system are used together with a matrixelement-based kinematic discriminant D_{ZZ^*}
- Signal and Z(Z*) estimated from MC expecion
- tXX and VVV estimated from MC expecion
- Z+jets and ttbar estimated from data-driven method
- No cut on the value of the BDT output applied, but the events are categorised in four exclusive equal-size BDT bins in order to better separate the signal from the background contribution in the m_H fit.

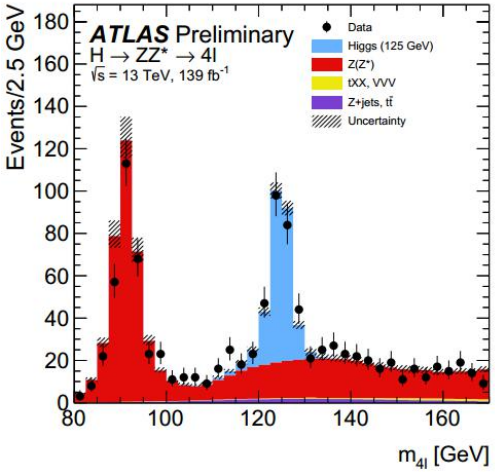

ATLAS-CONF-2020-005

D_{ZZ^*} is defined as $\ln(|\mathcal{M}_{HZZ^*}|^2/|\mathcal{M}_{ZZ^*}|^2)$

Higgs mass measurement

- An analytic model that takes into account the invariant mass resolution of the four-lepton system on a per-event basis is employed

- The mass of the Higgs boson has been measured from a fit to the invariant mass and the predicted invariant mass resolution of the H → Z Z* → 4l decay channel.

ATLAS-CONF-2020-005

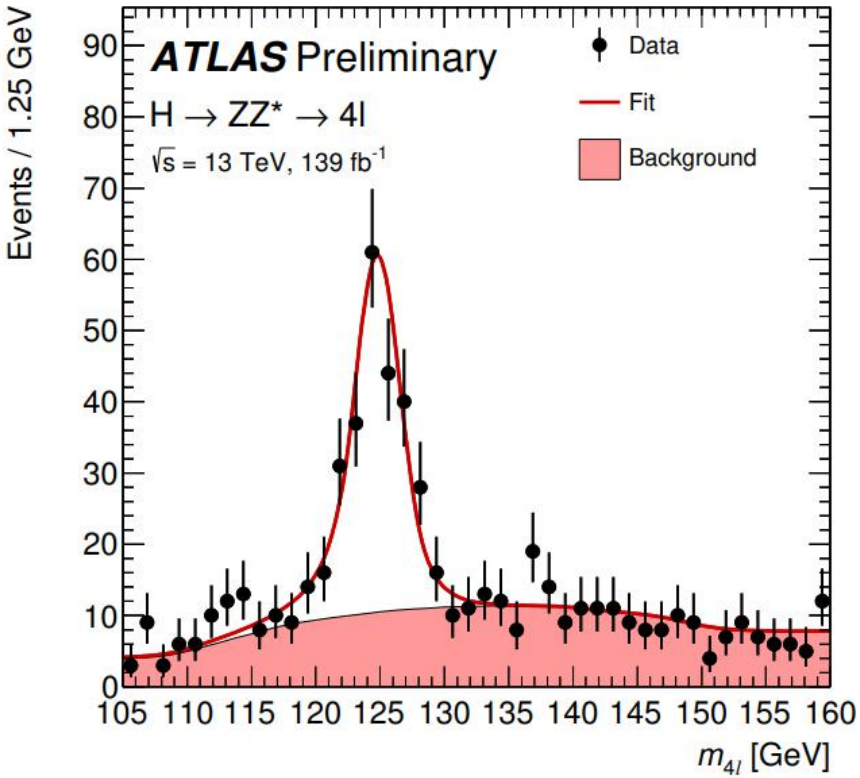

$$m_H = 124.92^{+0.21}_{-0.20}\ \text{GeV}$$

Impact of the leading systematic uncertainties on m_H

Systematic Uncertainty	Impact (GeV)
Muon momentum scale	+0.08,−0.06
Electron energy scale	±0.02
Muon momentum resolution	±0.01
Muon sagitta bias correction	±0.01

H→WW*: analysis

ATLAS-CONF-2021-014

Category	$N_{\text{jet},(p_T>30\text{ GeV})} = 0$ ggF	$N_{\text{jet},(p_T>30\text{ GeV})} = 1$ ggF	$N_{\text{jet},(p_T>30\text{ GeV})} \geq 2$ ggF	$N_{\text{jet},(p_T>30\text{ GeV})} \geq 2$ VBF
Preselection	Two isolated, different-flavour leptons ($\ell = e, \mu$) with opposite charge $p_T^{\text{lead}} > 22$ GeV , $p_T^{\text{sublead}} > 15$ GeV $m_{\ell\ell} > 10$ GeV			
	$p_T^{\text{miss}} > 20$ GeV			
Background rejection	$N_{b\text{-jet},(p_T>20\text{ GeV})} = 0$			
	$\Delta\phi_{\ell\ell,E_T^{\text{miss}}} > \pi/2$ $p_T^{\ell\ell} > 30$ GeV	$m_{\tau\tau} < m_Z - 25$ GeV		
		$\max(m_T^{\ell}) > 50$ GeV		
$H \to WW^* \to e\nu\mu\nu$ topology	$m_{\ell\ell} < 55$ GeV $\Delta\phi_{\ell\ell} < 1.8$			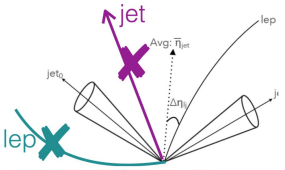 central jet veto outside lepton veto $m_{jj} > 120$ GeV
			fail central jet veto or fail outside lepton veto	
			$\lvert m_{jj} - 85\rvert > 15$ GeV or $\Delta y_{jj} > 1.2$	
Discriminant variable	m_T			DNN

H→WW*: analysis

ATLAS-CONF-2021-014

CR	$N_{\text{jet},(p_T>30\text{ GeV})} = 0$ ggF	$N_{\text{jet},(p_T>30\text{ GeV})} = 1$ ggF	$N_{\text{jet},(p_T>30\text{ GeV})} \geq 2$ ggF	$N_{\text{jet},(p_T>30\text{ GeV})} \geq 2$ VBF
$qq \to WW$	$N_{b\text{-jet},(p_T>20\text{ GeV})} = 0$			
	$55 < m_{\ell\ell} < 110$ GeV $\Delta\phi_{\ell\ell} < 2.6$	$m_{\ell\ell} > 80$ GeV		
		$\lvert m_{\tau\tau} - m_Z \rvert > 25$ GeV $\max(m_T^\ell) > 50$ GeV	$m_{\tau\tau} < m_Z - 25$ GeV $m_{T2} > 165$ GeV	
			fail central jet veto or fail outside lepton veto	
			$\lvert m_{jj} - 85 \rvert > 15$ GeV or $\Delta y_{jj} > 1.2$	
$t\bar{t}/Wt$	$N_{b\text{-jet},(20\text{ GeV}<p_T<30\text{ GeV})} > 0$ $\Delta\phi(\ell\ell, E_T^{\text{miss}}) > \pi/2$ $p_T^{\ell\ell} > 30$ GeV $\Delta\phi_{\ell\ell} < 2.8$	$N_{b\text{-jet},(p_T>30\text{ GeV})} = 1$ $N_{b\text{-jet},(20\text{ GeV}<p_T<30\text{ GeV})} = 0$	$N_{b\text{-jet},(p_T>20\text{ GeV})} = 0$	$N_{b\text{-jet},(p_T>20\text{ GeV})} = 1$
		$m_{\tau\tau} < m_Z - 25$ GeV		
		$\max(m_T^\ell) > 50$ GeV	$m_{\ell\ell} > 80$ GeV $\Delta\phi_{\ell\ell} < 1.8$ $m_{T2} < 165$ GeV	
			fail central jet veto or fail outside lepton veto	central jet veto outside lepton veto
			$\lvert m_{jj} - 85 \rvert > 15$ GeV or $\Delta y_{jj} > 1.2$	
Z/γ^*	$N_{b\text{-jet},(p_T>20\text{ GeV})} = 0$			
	$m_{\ell\ell} < 80$ GeV no p_T^{miss} requirement		$m_{\ell\ell} < 55$ GeV	$m_{\ell\ell} < 70$ GeV
	$\Delta\phi_{\ell\ell} > 2.8$	$m_{\tau\tau} > m_Z - 25$ GeV		$\lvert m_{\tau\tau} - m_Z \rvert \leq 25$ GeV central jet veto outside lepton veto
			fail central jet veto or fail outside lepton veto	
			$\lvert m_{jj} - 85 \rvert > 15$ GeV or $\Delta y_{jj} > 1.2$	

VBF ≥2 Jet: Deep Neural Network (DNN)

- More complex final state
- DNN inputs:

  (after preselection, $m_{\tau\tau} < m_Z - 25\,\text{GeV}$ & b-veto)

  m_{jj}, Δy_{jj}, $\sum_\ell C_\ell$ $(C_\ell = |2\eta_\ell - \sum \eta_j|/\Delta\eta_{jj})$

  $p_{\mathrm{T}}^{j0,j1,j2}$, $m_{\ell_i j_j}$, $m_{\ell\ell}$,

  $\Delta\phi_{\ell\ell}$, m_{T}, $p_{\mathrm{T}}^{\mathrm{tot}}$, $E_{\mathrm{T}}^{\mathrm{miss}}$ significance

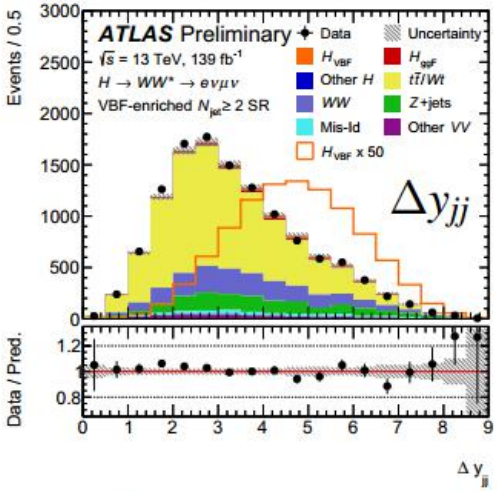

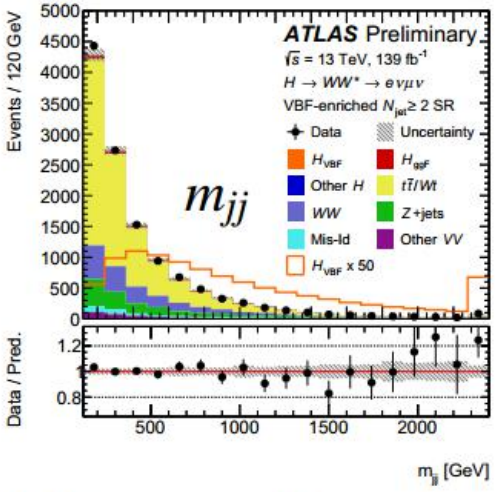

- Training target: VBF vs. non-H + ggF
  → reduce ggF/VBF interplay

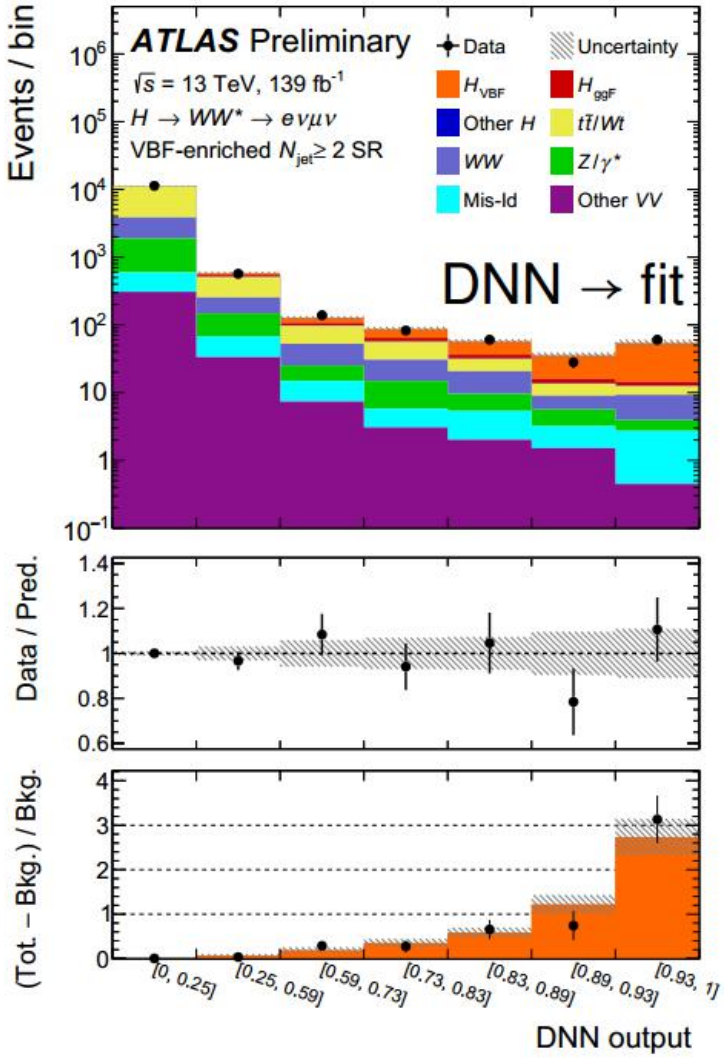

ATLAS-CONF-2021-014

H→WW*: analysis

ATLAS-CONF-2021-014

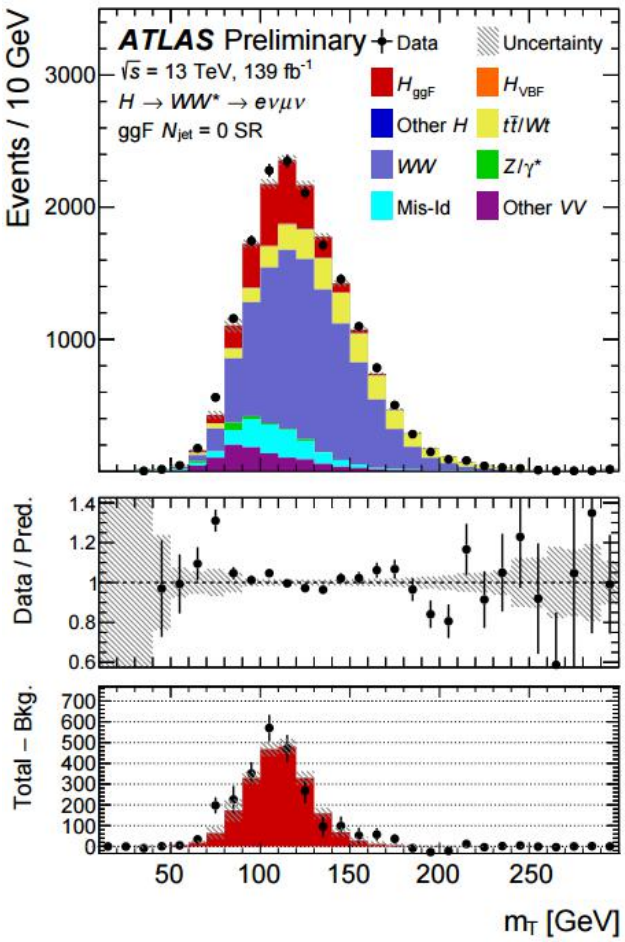

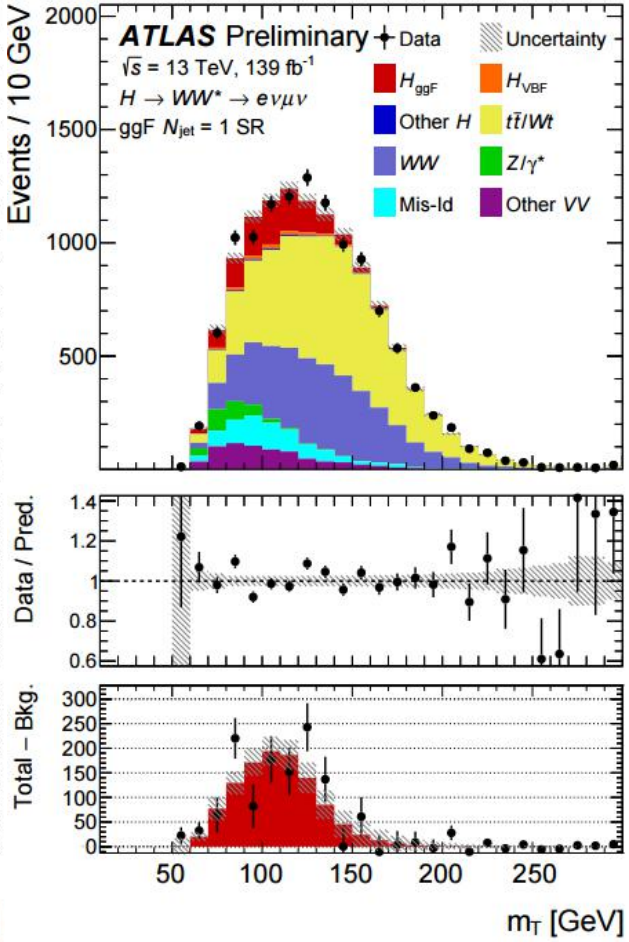

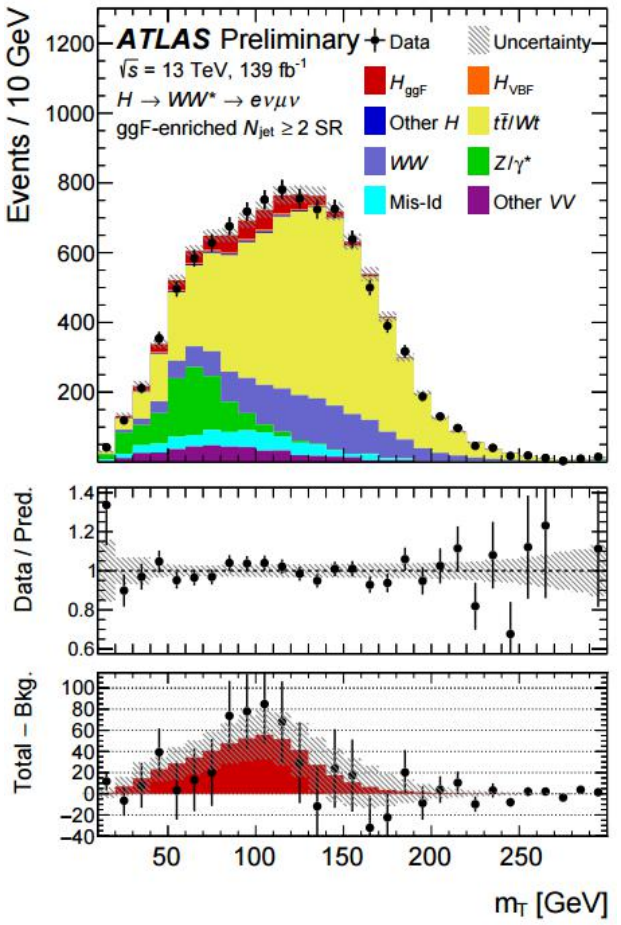

Break down

Source	$\frac{\Delta\sigma_{ggF}\cdot\mathcal{B}_{H\to WW^*}}{\sigma_{ggF}\cdot\mathcal{B}_{H\to WW^*}}$ [%]	$\frac{\Delta\sigma_{VBF}\cdot\mathcal{B}_{H\to WW^*}}{\sigma_{VBF}\cdot\mathcal{B}_{H\to WW^*}}$ [%]
Data statistical uncertainties	5	13
Total systematic uncertainties	11	18
MC statistical uncertainties	4	3.2
Experimental uncertainties	6	7
Flavour Tagging	2.4	0.9
Jet energy scale	1.4	3.3
Jet energy resolution	2.3	1.9
$E_{\mathrm{T}}^{\mathrm{miss}}$	1.9	5
Muons	2.1	0.7
Electrons	1.5	0.3
Fake factors	2.4	1.0
Pile-up	2.4	1.3
Luminosity	2.0	2.1
Theoretical uncertainties	8	16
ggF	5	4
VBF	0.7	13
Top	4	5
$Z\tau\tau$	2.0	2.1
WW	4	5
Other VV	3	1.2
Background normalisations	5	5
WW	3.1	0.5
Top	2.4	2.2
$Z\tau\tau$	3.1	4
TOTAL	12	22

H→WW*: STXS

ATLAS-CONF-2021-014

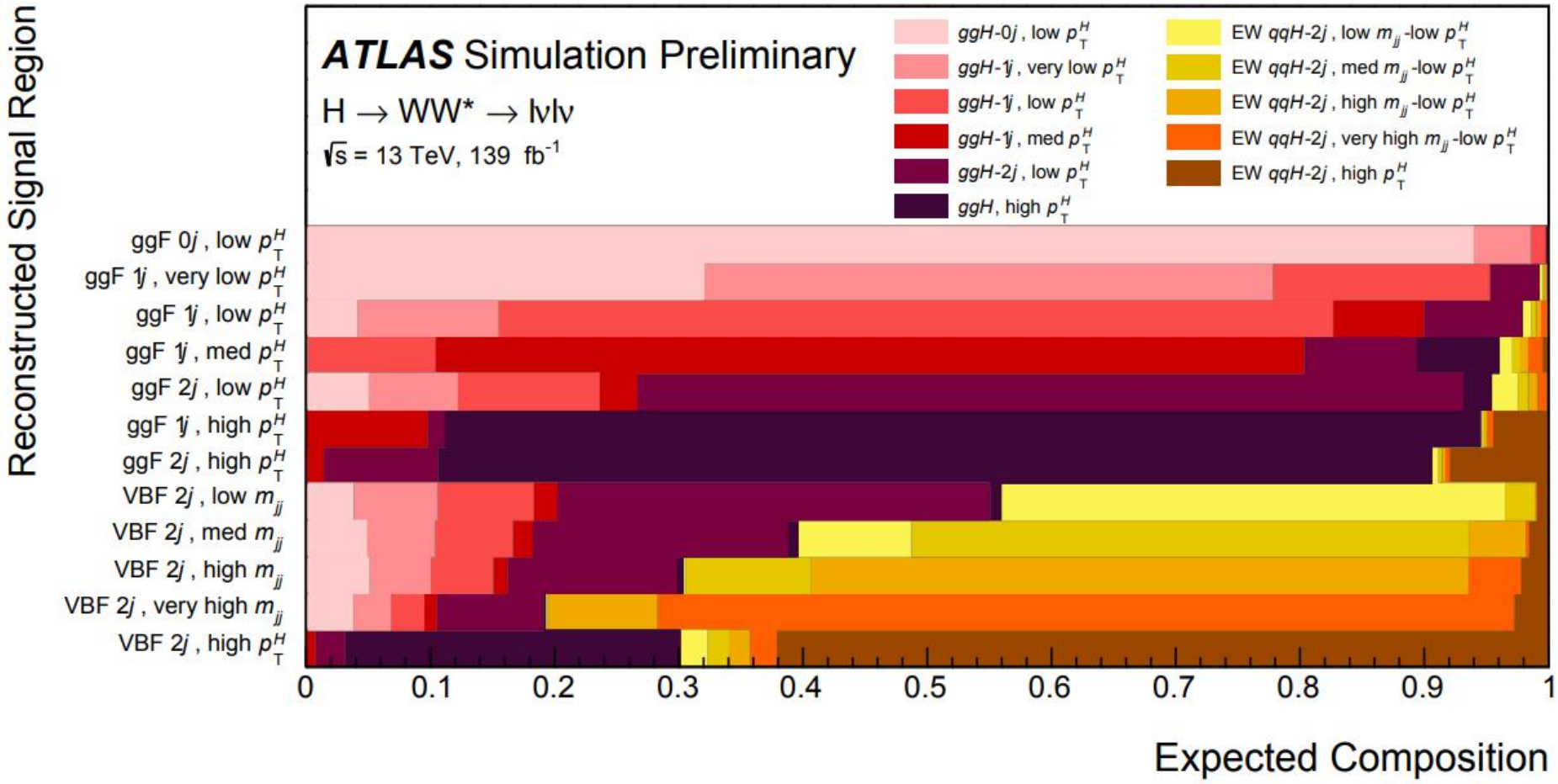

H→WW*: STXS

ATLAS-CONF-2021-014

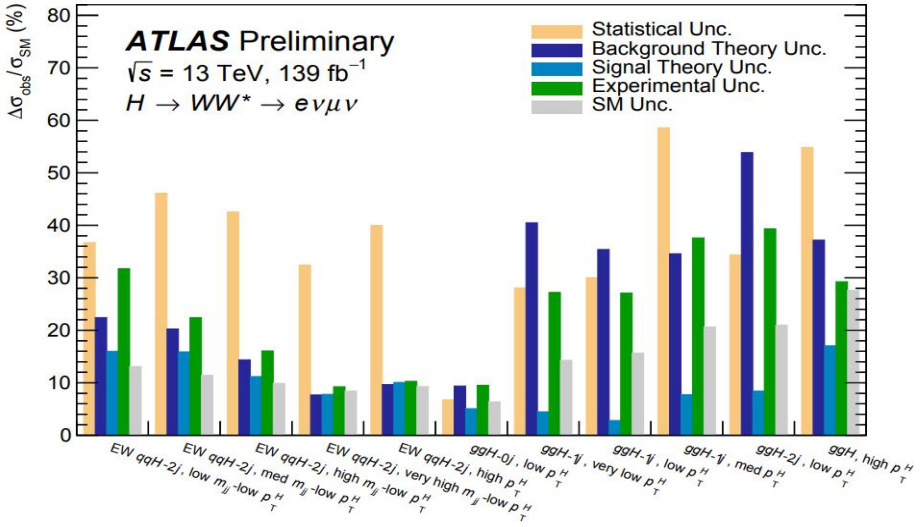

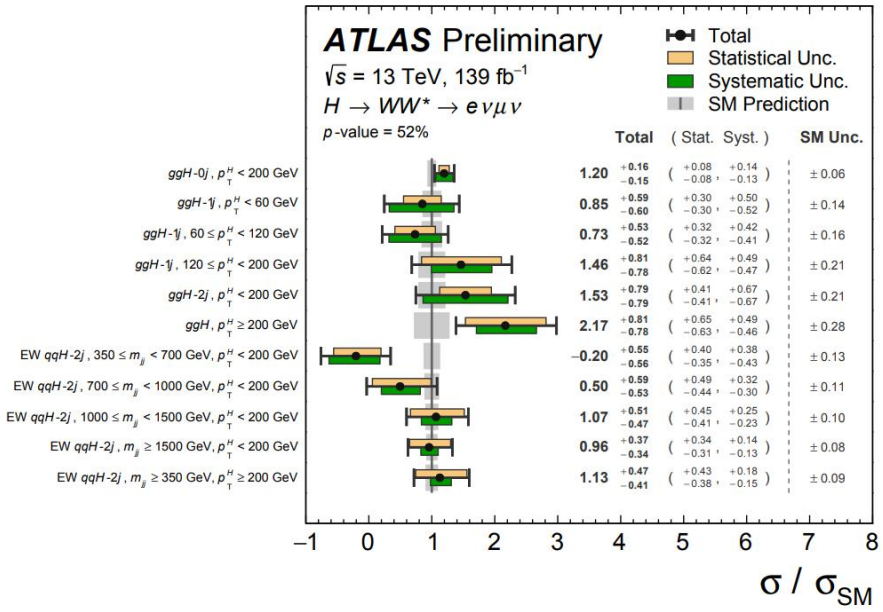

STXS category ($\sigma_i \times B_{WW}$)	Value [fb]	Uncertainty [fb] Total	Stat.	Exp. Syst.	Sig. Theo.	Bkg. Theo.	SM prediction [fb]
ggH-0j, low p_T^H p_T^H < 200 GeV	7000	$^{+900}_{-900}$	$^{+400}_{-400}$	$^{+600}_{-500}$	$^{+300}_{-300}$	$^{+600}_{-500}$	5900 ± 400
ggH-1j, very low p_T^H p_T^H < 60 GeV	1190	$^{+820}_{-840}$	$^{+390}_{-390}$	$^{+380}_{-380}$	$^{+70}_{-60}$	$^{+550}_{-580}$	1400 ± 200
ggH-1j, low p_T^H 60 ≤ p_T^H < 120 GeV	710	$^{+510}_{-510}$	$^{+290}_{-290}$	$^{+270}_{-260}$	$^{+30}_{-30}$	$^{+340}_{-340}$	970 ± 150
ggH-1j, med p_T^H 120 ≤ p_T^H < 200 GeV	230	$^{+130}_{-120}$	$^{+90}_{-90}$	$^{+60}_{-60}$	$^{+10}_{-10}$	$^{+60}_{-50}$	160 ± 30
ggH-2j, low p_T^H p_T^H < 200 GeV	1560	$^{+800}_{-800}$	$^{+350}_{-350}$	$^{+400}_{-400}$	$^{+90}_{-80}$	$^{+550}_{-540}$	1010 ± 210
ggH, high p_T^H p_T^H ≥ 200 GeV	270	$^{+100}_{-100}$	$^{+70}_{-70}$	$^{+40}_{-40}$	$^{+30}_{-10}$	$^{+50}_{-40}$	122 ± 34
EW qqH-2j, low m_{jj}-low p_T^H 350 ≤ m_{jj} < 700 GeV, p_T^H < 200 GeV	−20	$^{+60}_{-60}$	$^{+40}_{-40}$	$^{+30}_{-40}$	$^{+10}_{-20}$	$^{+20}_{-30}$	109 ± 14
EW qqH-2j, med m_{jj}-low p_T^H 700 ≤ m_{jj} < 1000 GeV, p_T^H < 200 GeV	28	$^{+33}_{-30}$	$^{+27}_{-24}$	$^{+12}_{-13}$	$^{+10}_{-8}$	$^{+11}_{-11}$	56 ± 6
EW qqH-2j, high m_{jj}-low p_T^H 1000 ≤ m_{jj} < 1500 GeV, p_T^H < 200 GeV	54	$^{+26}_{-24}$	$^{+23}_{-20}$	$^{+8}_{-8}$	$^{+7}_{-5}$	$^{+7}_{-7}$	51 ± 5
EW qqH-2j, very high m_{jj}-low p_T^H m_{jj} ≥ 1500 GeV, p_T^H < 200 GeV	48	$^{+19}_{-17}$	$^{+17}_{-15}$	$^{+5}_{-5}$	$^{+5}_{-3}$	$^{+4}_{-4}$	50 ± 4
EW qqH-2j, high p_T^H m_{jj} ≥ 350 GeV, p_T^H ≥ 200 GeV	36	$^{+15}_{-13}$	$^{+13}_{-12}$	$^{+3}_{-3}$	$^{+4}_{-3}$	$^{+3}_{-3}$	32 ± 3

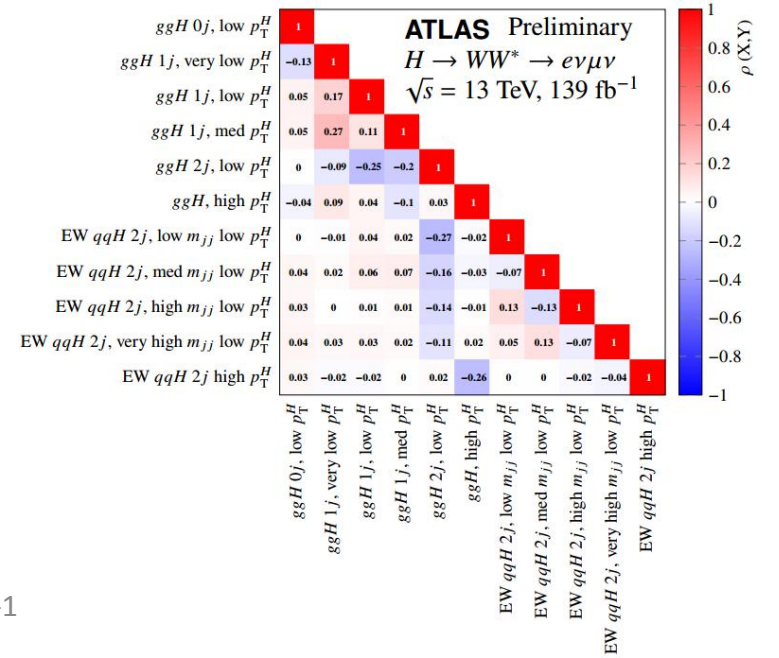

H→ZZ*: STXS

Eur. Phys. J. C 80, 957 (2020).

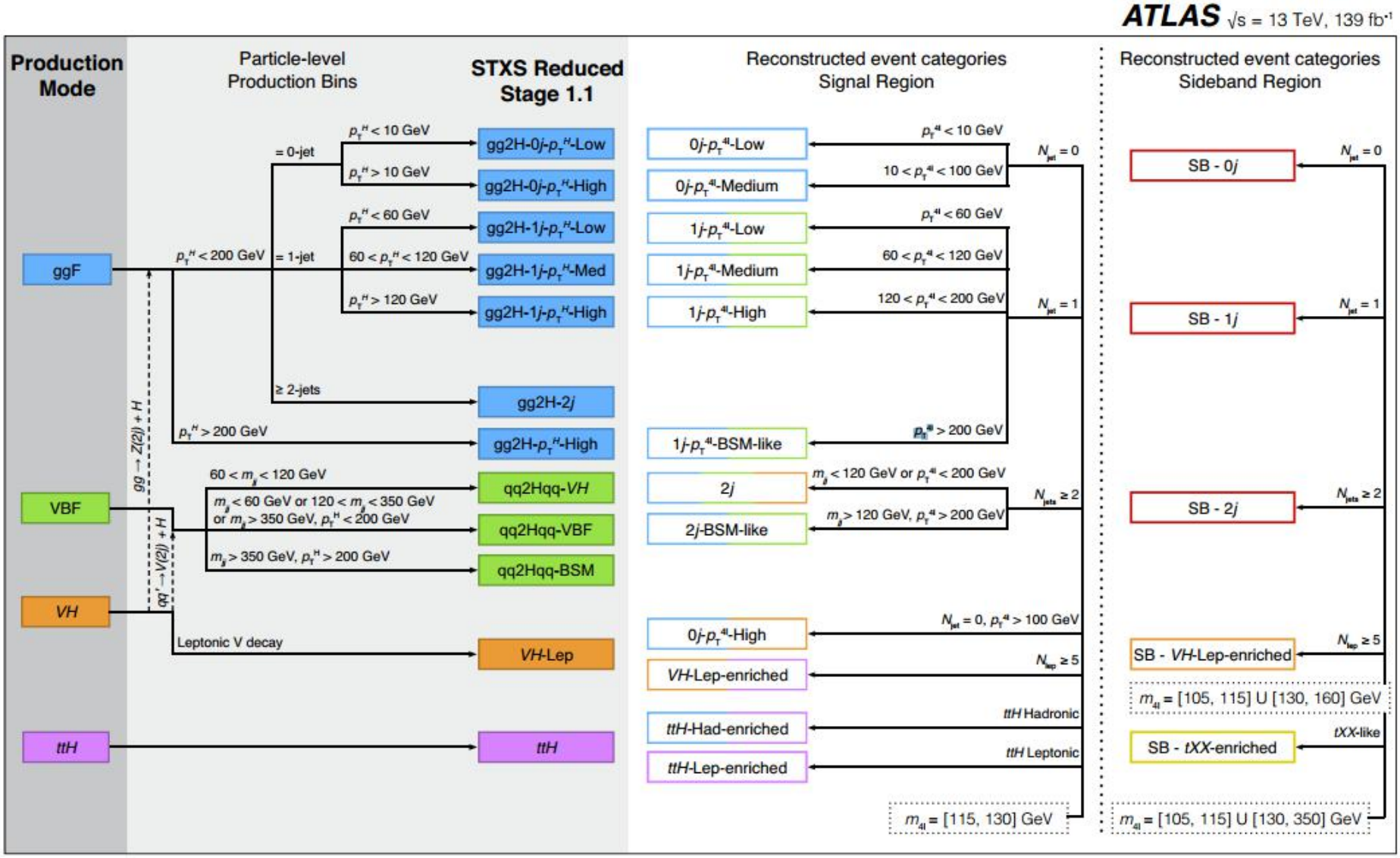

H→ZZ*: STXS

Eur. Phys. J. C 80, 957 (2020).

- Two types of NNs are used: feed-forward multilayer perceptron (MLP) and recurrent (RNN)
- The input variables used to train the MLP, and the two RNNs for the four leptons and the jets

Category	Processes	MLP	Lepton RNN	Jet RNN	Discriminant
$0j$-$p_{\mathrm{T}}^{4\ell}$-Low $0j$-$p_{\mathrm{T}}^{4\ell}$-Med	ggF, ZZ^*	$p_{\mathrm{T}}^{4\ell}$, D_{ZZ^*}, m_{12}, m_{34}, $\lvert\cos\theta^*\rvert$, $\cos\theta_1$, ϕ_{ZZ}	p_{T}^{ℓ}, η_{ℓ}	-	$\mathrm{NN}_{\mathrm{ggF}}$
$1j$-$p_{\mathrm{T}}^{4\ell}$-Low	ggF, VBF, ZZ^*	$p_{\mathrm{T}}^{4\ell}$, p_{T}^{j}, η_j, $\Delta R_{4\ell j}$, D_{ZZ^*}	p_{T}^{ℓ}, η_{ℓ}	-	$\mathrm{NN}_{\mathrm{VBF}}$ for $\mathrm{NN}_{ZZ} < 0.25$ NN_{ZZ} for $\mathrm{NN}_{ZZ} > 0.25$
$1j$-$p_{\mathrm{T}}^{4\ell}$-Med	ggF, VBF, ZZ^*	$p_{\mathrm{T}}^{4\ell}$, p_{T}^{j}, η_j, $E_{\mathrm{T}}^{\mathrm{miss}}$, $\Delta R_{4\ell j}$, D_{ZZ^*}, $\eta_{4\ell}$	p_{T}^{ℓ}, η_{ℓ}	-	$\mathrm{NN}_{\mathrm{VBF}}$ for $\mathrm{NN}_{ZZ} < 0.25$ NN_{ZZ} for $\mathrm{NN}_{ZZ} > 0.25$
$1j$-$p_{\mathrm{T}}^{4\ell}$-High	ggF, VBF	$p_{\mathrm{T}}^{4\ell}$, p_{T}^{j}, η_j, $E_{\mathrm{T}}^{\mathrm{miss}}$, $\Delta R_{4\ell j}$, $\eta_{4\ell}$	p_{T}^{ℓ}, η_{ℓ}	-	$\mathrm{NN}_{\mathrm{VBF}}$
$2j$	ggF, VBF, VH	m_{jj}, $p_{\mathrm{T}}^{4\ell jj}$	p_{T}^{ℓ}, η_{ℓ}	p_{T}^{j}, η_j	$\mathrm{NN}_{\mathrm{VBF}}$ for $\mathrm{NN}_{VH} < 0.2$ NN_{VH} for $\mathrm{NN}_{VH} > 0.2$
$2j$-BSM-like	ggF, VBF	$\eta_{ZZ}^{\mathrm{Zepp}}$, $p_{\mathrm{T}}^{4\ell jj}$	p_{T}^{ℓ}, η_{ℓ}	p_{T}^{j}, η_j	$\mathrm{NN}_{\mathrm{VBF}}$
VH-Lep-enriched	VH, ttH	N_{jets}, $N_{b\text{-jets},70\%}$, $E_{\mathrm{T}}^{\mathrm{miss}}$, H_{T}	p_{T}^{ℓ}	-	NN_{ttH}
ttH-Had-enriched	ggF, ttH, tXX	$p_{\mathrm{T}}^{4\ell}$, m_{jj}, $\Delta R_{4\ell j}$, $N_{b\text{-jets},70\%}$,	p_{T}^{ℓ}, η_{ℓ}	p_{T}^{j}, η_j	NN_{ttH} for $\mathrm{NN}_{tXX} < 0.4$ NN_{tXX} for $\mathrm{NN}_{tXX} > 0.4$

H→ZZ*: STXS

Eur. Phys. J. C 80, 957 (2020).

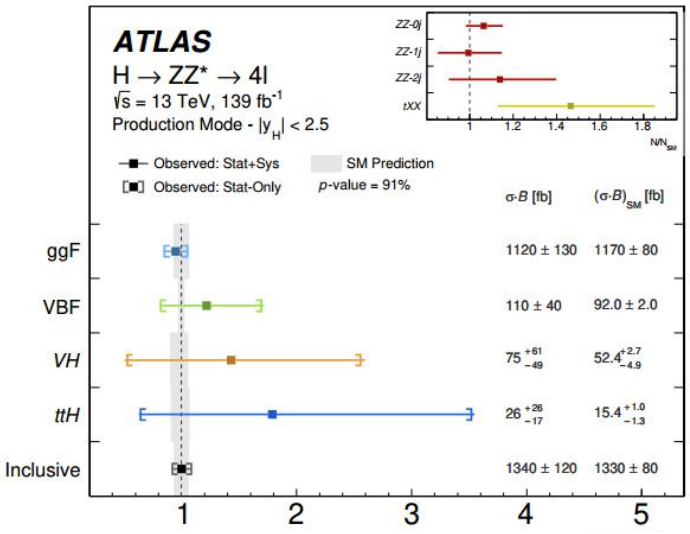

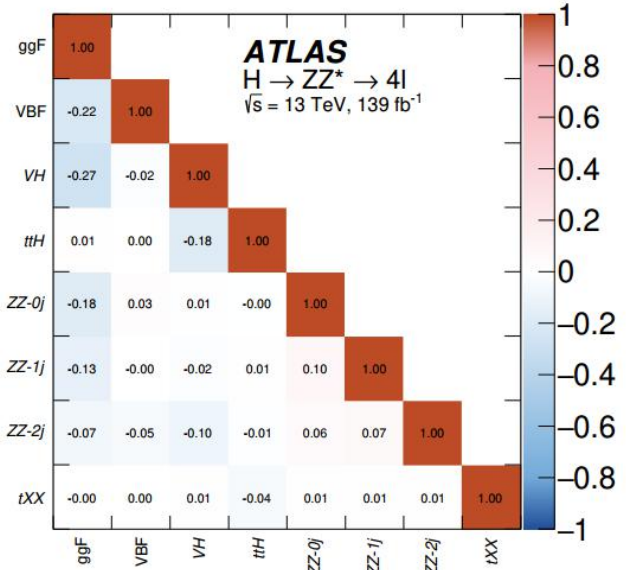

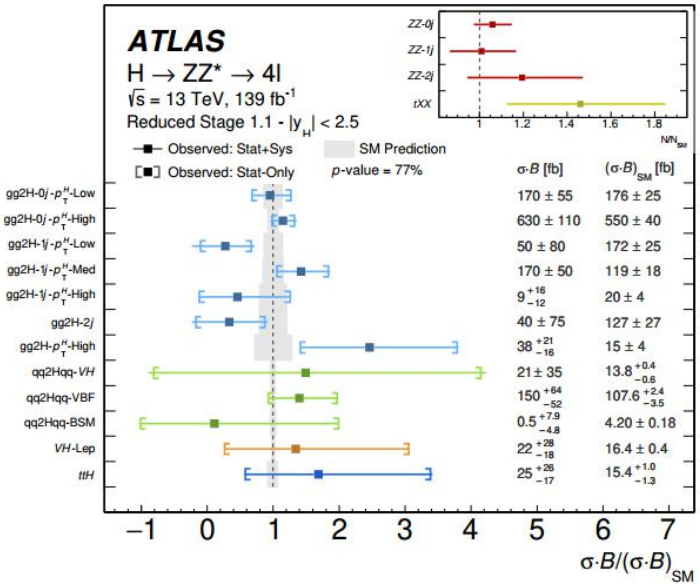

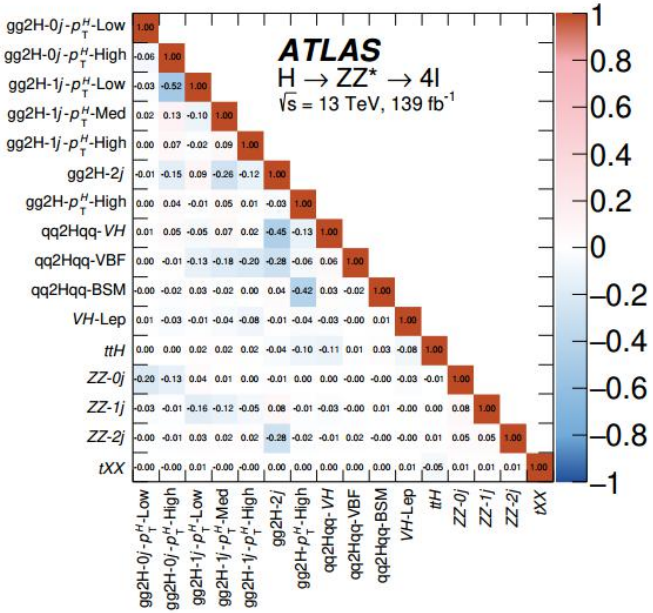

H→ZZ*: STXS

Eur. Phys. J. C 80, 957 (2020).

Measurement	Experimental uncertainties [%]				Theory uncertainties [%]				
	Lumi.	e, μ, pile-up	Jets, flav. tag	Reducible bkg	Background ZZ^*	Background tXX	Signal PDF	Signal QCD	Signal Shower
Inclusive cross-section									
	1.7	2.5	0.5	< 0.5	1	< 0.5	< 0.5	1	2
Production mode cross-sections									
ggF	1.7	2.5	1	< 0.5	1.5	< 0.5	0.5	1	2
VBF	1.7	2	4	< 0.5	1.5	< 0.5	1	5	7
VH	1.9	2	4	1	6	< 0.5	2	13.5	7.5
ttH	1.7	2	6	< 0.5	1	0.5	0.5	12.5	4
Reduced Stage-1.1 production bin cross-sections									
gg2H-0j-p_{T}^{H}-Low	1.7	3	1.5	0.5	6.5	< 0.5	< 0.5	1	1.5
gg2H-0j-p_{T}^{H}-High	1.7	3	5	< 0.5	3	< 0.5	< 0.5	0.5	5.5
gg2H-1j-p_{T}^{H}-Low	1.7	2.5	12	0.5	7	< 0.5	< 0.5	1	6
gg2H-1j-p_{T}^{H}-Med	1.7	3	7.5	< 0.5	1	< 0.5	< 0.5	1.5	5.5
gg2H-1j-p_{T}^{H}-High	1.7	3	11	0.5	2	< 0.5	< 0.5	2	7.5
gg2H-2j	1.7	2.5	16.5	1	12.5	0.5	< 0.5	2.5	10.5
gg2H-p_{T}^{H}-High	1.7	1.5	3	0.5	3.5	< 0.5	< 0.5	2	3.5
qq2Hqq-VH	1.8	4	17	1	4	1	0.5	5.5	8
qq2Hqq-VBF	1.7	2	3.5	< 0.5	5	< 0.5	< 0.5	6	10.5
qq2Hqq-BSM	1.7	2	4	< 0.5	2.5	< 0.5	< 0.5	3	8
VH-Lep	1.8	2.5	2	1	2	0.5	< 0.5	1.5	3
ttH	1.7	2.5	5	0.5	1	0.5	< 0.5	11	3

- the luminosity uncertainty, which is measured to be 1.7% and increases for the VH signal processes due to the simulation-based normalisation of the background.

$H \to \gamma\gamma$: STXS

ATLAS-CONF-2020-026

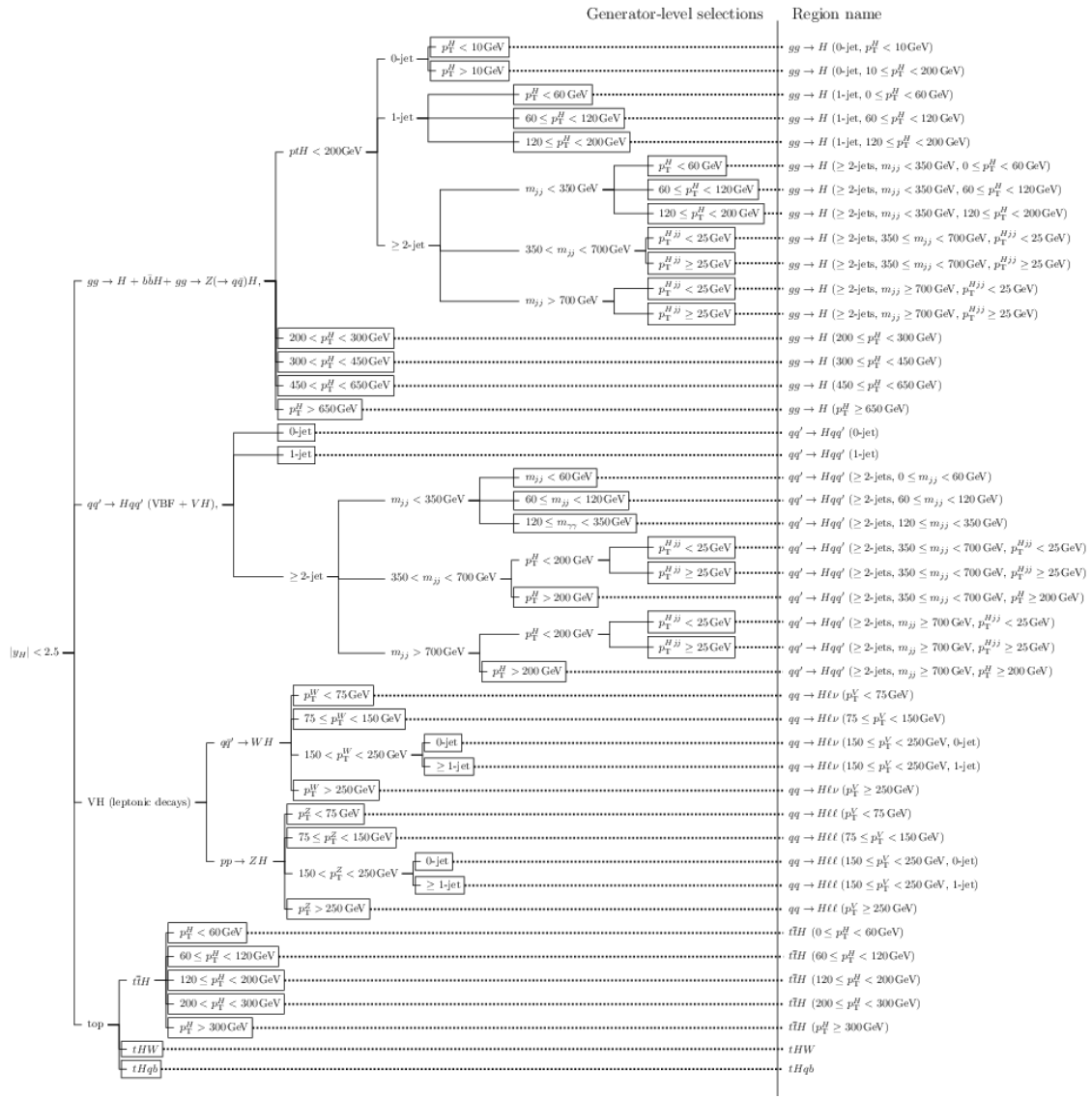

H→γγ: Production Mode Cross Sections

ATLAS-CONF-2020-026

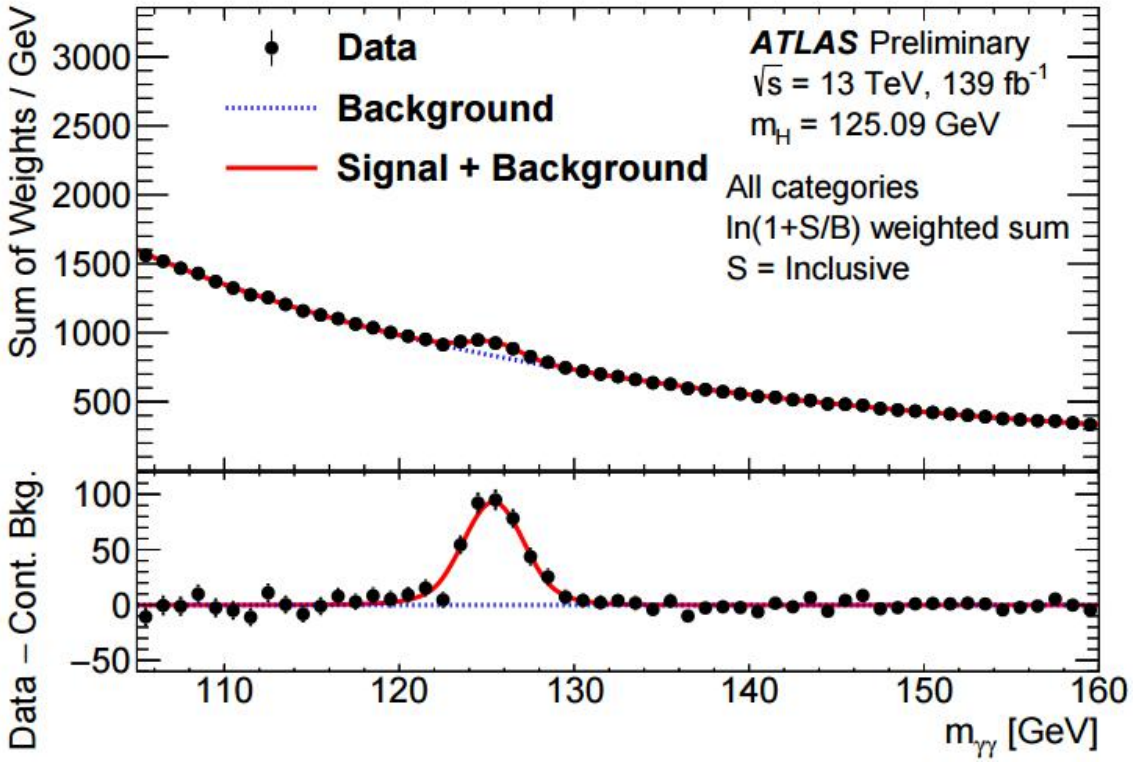

The events in each category are weighted by ln(1+S/B)

The fitted signal plus background PDFs from all categories are also weighted and summed

- This choice of event weight is designed to enhance the contribution of events from categories with higher signal-to-background ratio in a way that approximately matches the impact of these events in the categorized analysis of the data

H→γγ: Production Mode Cross Sections

ATLAS-CONF-2020-026

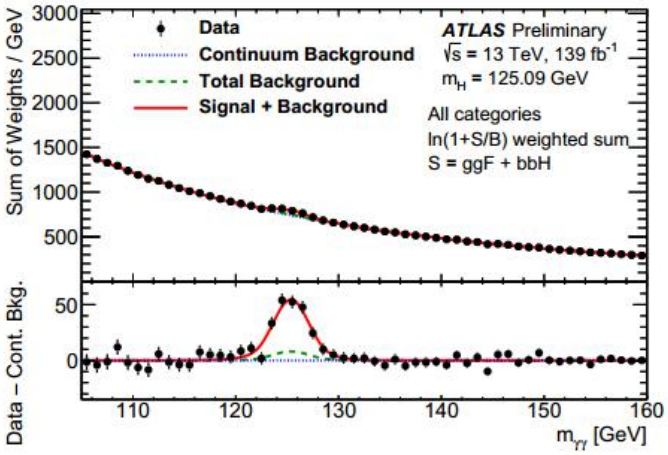

(a) ggF+ $b\bar{b}H$

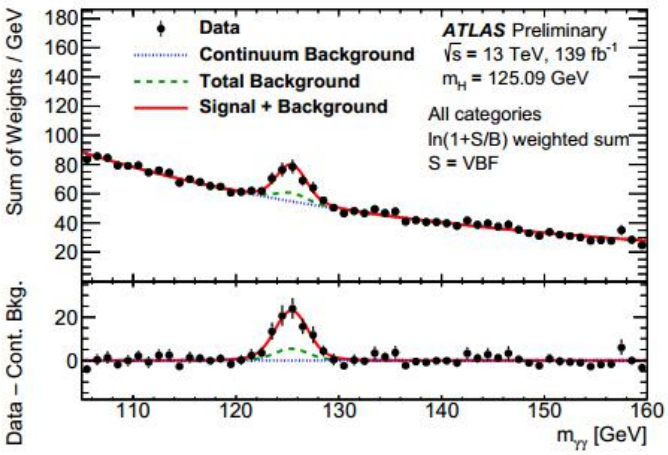

(b) VBF

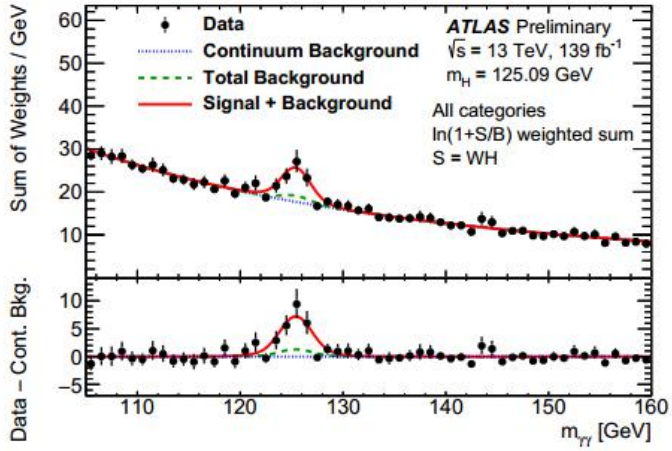

(c) WH

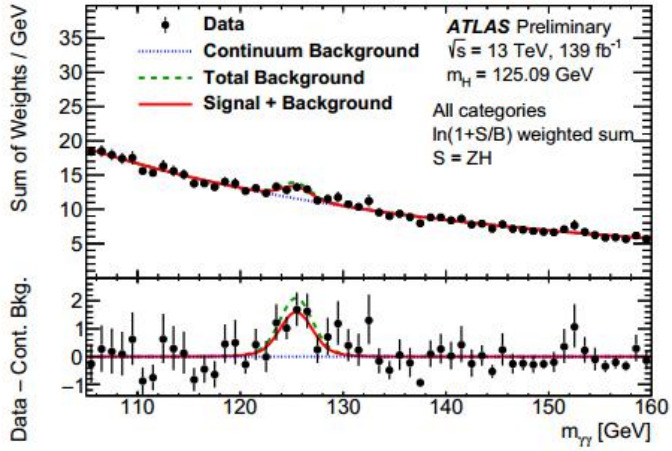

(d) ZH

H→γγ: Production Mode Cross Sections (breakdown)

ATLAS-CONF-2020-026

Uncertainty source	ggF+ $b\bar{b}H$ $\Delta\sigma$[%]	VBF $\Delta\sigma$[%]	WH $\Delta\sigma$[%]	ZH $\Delta\sigma$[%]	$t\bar{t}H + tH$ $\Delta\sigma$[%]
Underlying Event and Parton Shower (UEPS)	±2.3	±10	< ±1	±9.6	±3.5
Modeling of Heavy Flavor Jets in non-$t\bar{t}H$ Processes	< ±1	< ±1	< ±1	< ±1	±1.3
Higher-Order QCD Terms (QCD)	±1.6	< ±1	< ±1	±1.9	< ±1
Parton Distribution Function and α_S Scale (PDF+α_S)	< ±1	±1.1	< ±1	±1.9	< ±1
Photon Energy Resolution (PER)	±2.9	±2.4	±2.0	±1.3	±4.9
Photon Energy Scale (PES)	< ±1	< ±1	< ±1	±3.4	±2.2
Jet/$E_{\mathrm{T}}^{\mathrm{miss}}$	±1.6	±5.5	±1.2	±4.0	±3.0
Photon Efficiency	±2.5	±2.3	±2.4	±1.4	±2.4
Background Modeling	±4.1	±4.7	±2.8	±18	±2.4
Flavor Tagging	< ±1	< ±1	< ±1	< ±1	< ±1
Leptons	< ±1	< ±1	< ±1	< ±1	< ±1
Pileup	±1.8	±2.7	±2.1	±3.8	±1.1
Luminosity and Trigger	±2.1	±2.1	±2.3	±1.1	±2.3
Higgs Boson Mass	< ±1	< ±1	< ±1	±3.7	±1.9

H→γγ: Production Mode Cross Sections

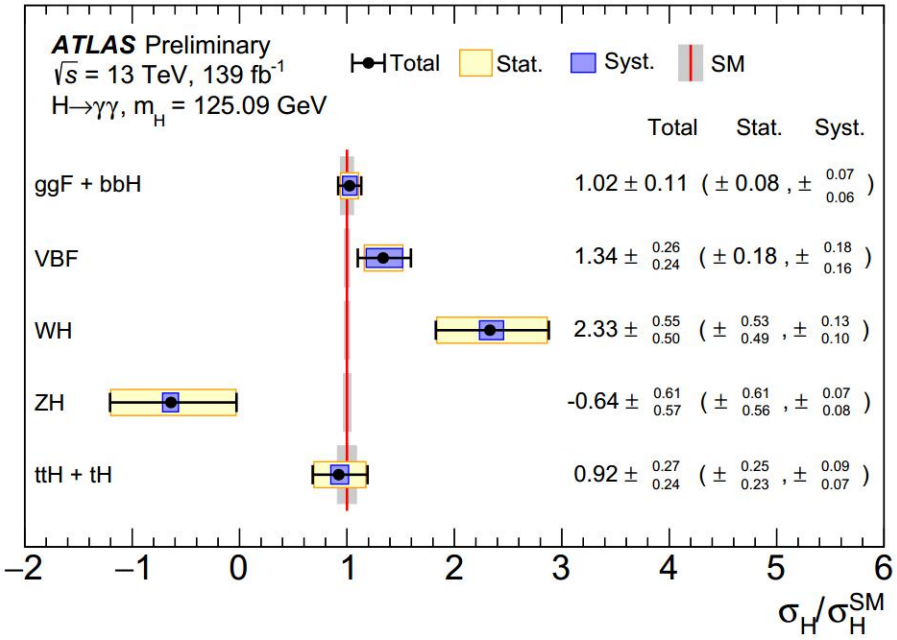

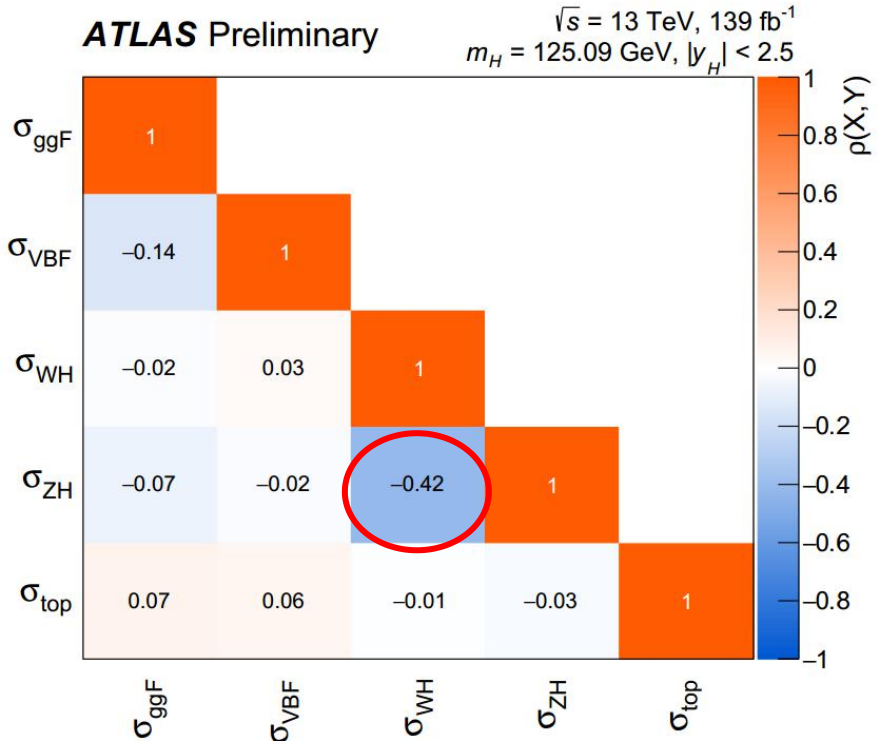

$H \to \gamma\gamma$: STXS (27 pois)

ATLAS-CONF-2020-026

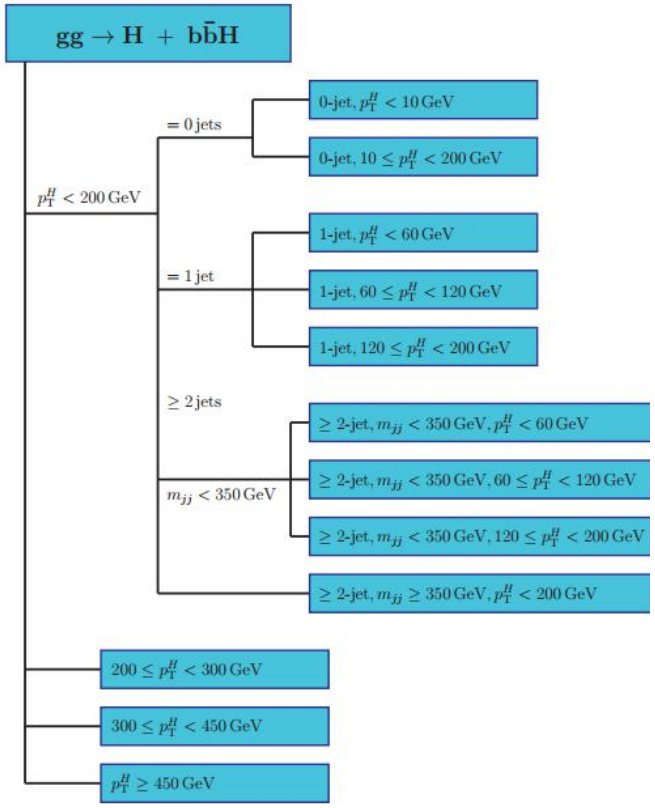

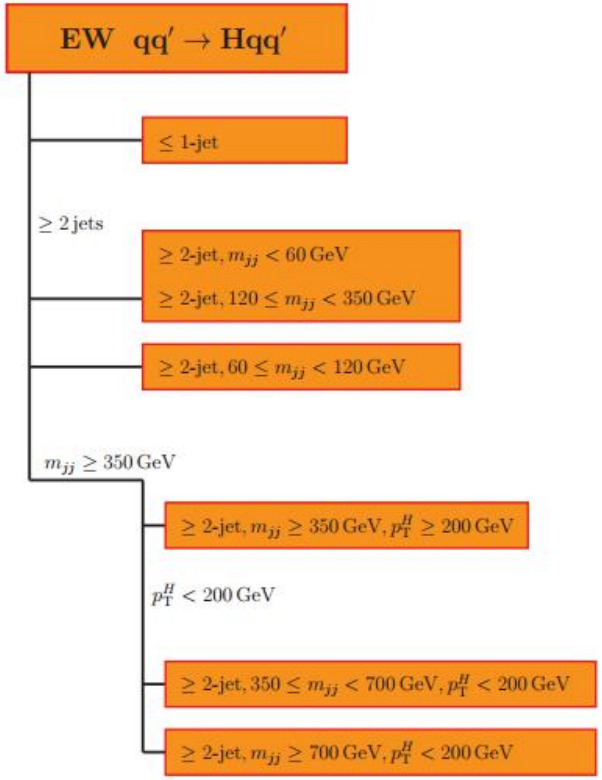

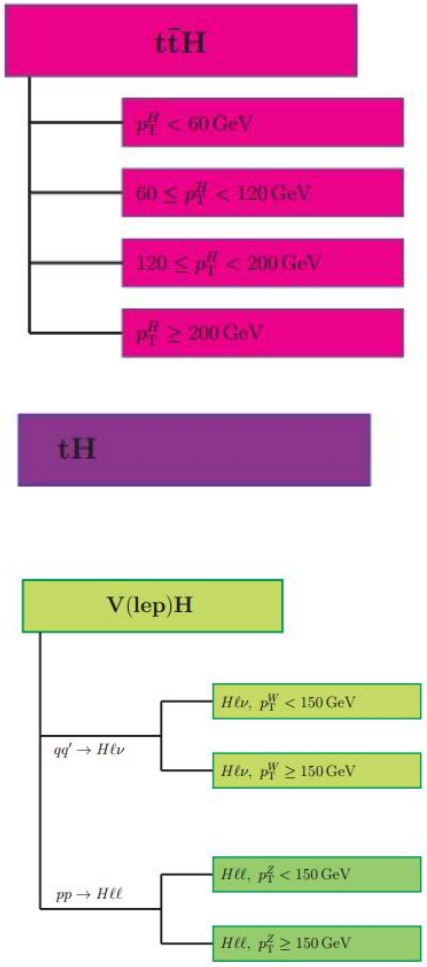

H→ZZ*→4ℓ: Inclusive and Differential Cross Section

Eur. Phys. J. C 80, 942 (2020)

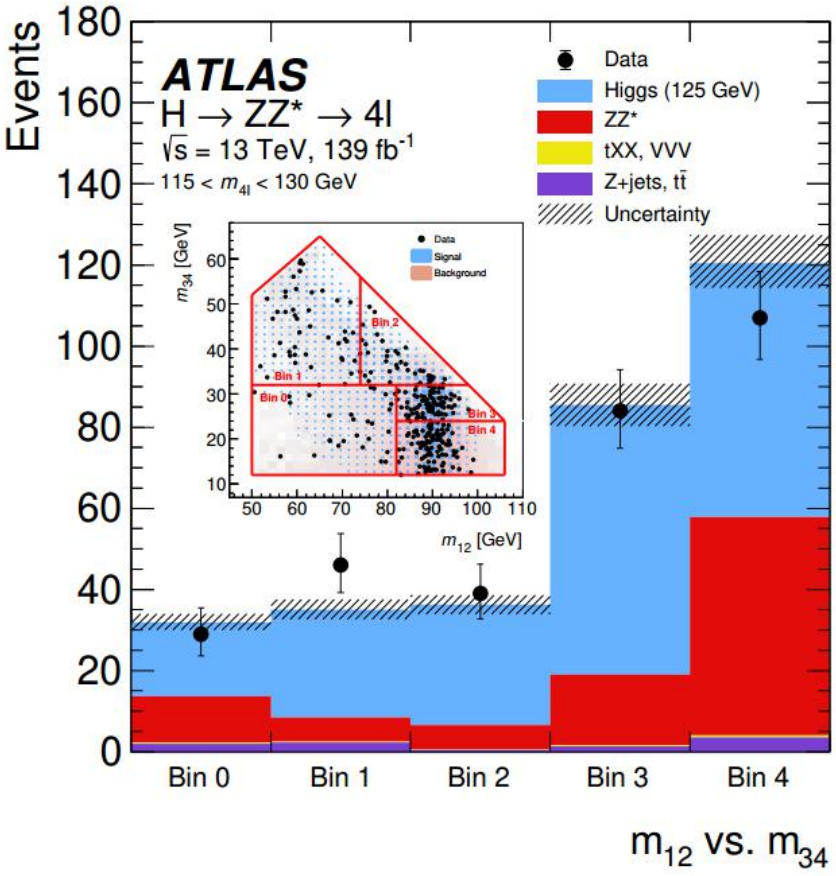

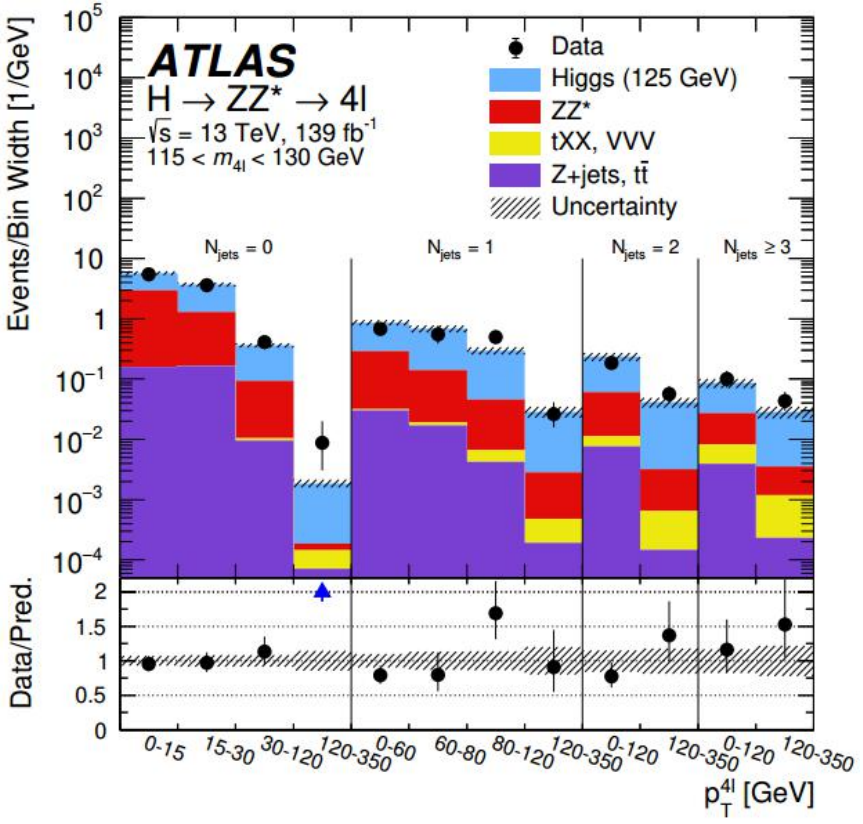

H→ZZ*→4ℓ: Inclusive and Differential Cross Section
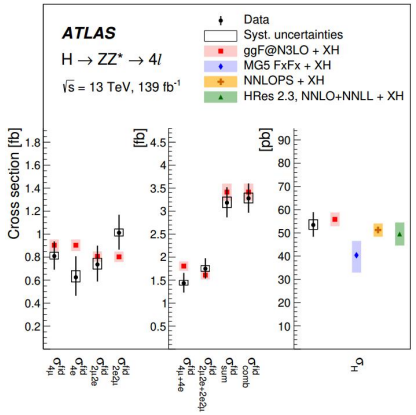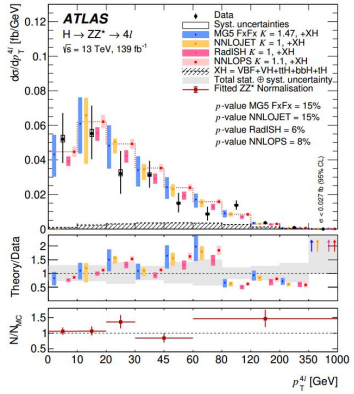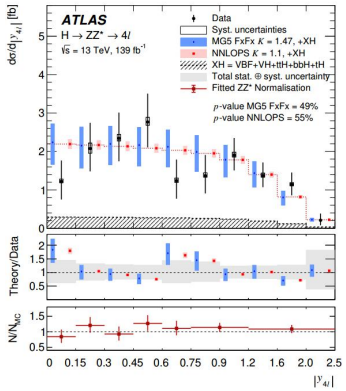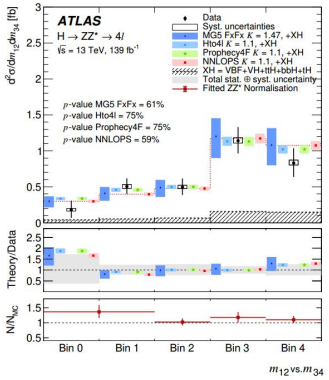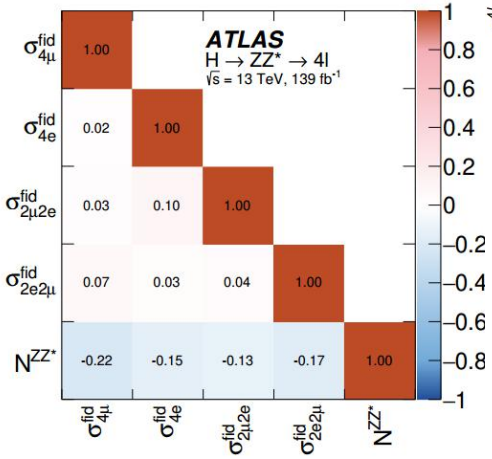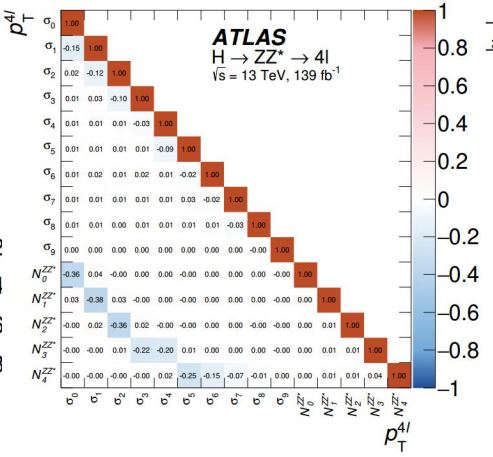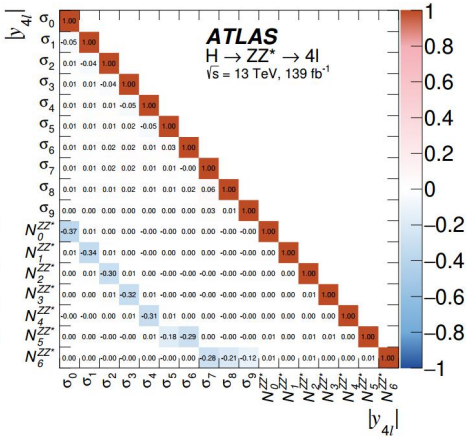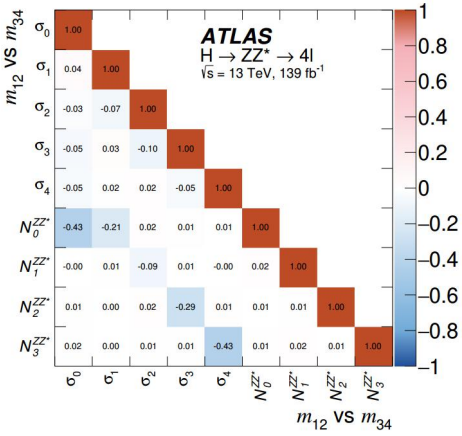
Eur. Phys. J. C 80, 942 (2020)